이학박사 학위논문

Development of anti-cotinine antibody & its application to EIA and carrier for cotinine-conjugated molecule

항 코티닌 항체의 개발과 효소면역측정법 및 코티닌 접합물질에 대한 운반체로의 적용

2012년 8월

서울대학교 대학원

의학과 생화학 전공

박 선 영

Contents

Introduction

Ⅰ. Cotinine

Cotinine is an alkaloid $C_{10}H_{12}N_2O$ that is the principal metabolite of nicotine and has been widely used as a tobacco biomarker (Fig. 1). Since cotinine has a much longer serum half-life than nicotine (approximately 20 h compare to 2 h for nicotine) (Benowitz *et al*., 2009), it is retained in the body for a considerable period of time (up to one week) after the use of tobacco. Thus, cotinine can be detected in a number of biological fluids including serum, saliva, urine, serume and cervical exudates, and is used to assess an individual's exposure to tobacco smoke exposure, including passive smoke.

Nicotine is a key component of tobacco smoke, and it has a number of neuroregulatory influences. Oral snuff and pipe tobacco contain concentrations of nicotine similar to cigarette tobacco, whereas cigar and chewing tobacco have only about half the nicotine concentration of cigarette tobacco. An average tobacco rod contains 10-14 mg of nicotine (Kozlowski *et al.*, 1998), and on average about 1-1.5 mg of nicotine is absorbed systemically during smoking (Benowitz and Jacob, 1984). As nicotine is entered the body by inhalation, it is absorbed into the bloodstream and crossed the blood-brain barrier reaching the brain within 10-20 seconds (Perry *et al.*, 1999). The rapid rate of delivery of nicotine by smoking results in high levels of nicotine in the central nervous system with little time for development of tolerance. The result is a more intense pharmacologic action. The short time interval between puffing and nicotine entering the brain also allows

the smoker to titrate the dose of nicotine to a desired pharmacologic effect, further reinforcing drug self-administration and facilitating the development of addiction. In the liver, nicotine is extensively metabolized to a number of metabolites primarily by oxidation systems (C-, N-oxidation). A small percentage, usually 5-10%, of nicotine is excreted unchanged into the urine. Six primary metabolites of nicotine have been identified: cotinine, nicotine N-oxide, nornicotine, nicotine glucuronide, nicotine isomethonium ion and 2′-hydroxynicotine (Fig. 1).

Cotinine is the most important product of the C-oxidation pathway of nicotine in most mammalian species. In humans, about 70–80% of nicotine is converted to cotinine. This transformation involves double-step oxidation of nicotine. The first is mediated primarily by cytochrome p450 2A6 (CYP2A6) to produce nicotine-$\Delta^{1'(5')}$-iminium ion, which is in equilibrium with 5′-hydroxynicotine. The second step is oxidation of the iminium ion intermediate to cotinine catalyzed by a cytoplasmic aldehyde oxidase (Shigenaga *et al.*, 1988) (Fig. 2). Only 10-15% of cotinine itself is excreted in the urine (Benowitz et al., 1994). The remainder of the cotinine is converted to other metabolites, particularly trans-3'-hydroxycotinine, cotinine glucuronide, and cotinine N-oxide. 3′-hydroxycotinine is converted by C-oxidation of cotinine and the main nicotine metabolite detected in smokers' urine. It is also excreted as a glucuronide conjugate. 3′-hydroxycotinine and its glucuronide conjugate account for 40–60% of the nicotine dose in urine (Benowitz et al., 1994). Recently trans-3′-hydroxycotinine has assumed a significant role in nicotine metabolism. Although C-oxidation is the major pathway of nicotine metabolism, N-oxidation pathway catalyzed by flavin-containing monooxygenase 3 (FMO3) (Benowitz

et al., 1994) and two nonoxidative pathways including methylation and glucuronidation pathway catalyzed by uridine diphosphateglucuronosyltransferase (UGT) (Benowitz et al., 1994) involved in nicotine metabolism (Fig. 1).

Nicotine is rapidly metabolized and has a short half-life, but cotinine is metabolized and eliminated at a much lower rate. Cotinine assays provide an objective quantitative measure that is more reliable than smoking histories or counting the number of cigarettes smoked per day. Today medical studies have proven that smoking tobacco is among the leading causes of many diseases such as lung cancer, heart attacks, erectile dysfunction and can also lead to birth defects. The inherent health hazards of smoking have caused many countries to institute high taxes on tobacco products and anti-smoking campaigns are launched every year in an attempt to curb tobacco smoking. Also, due to the severe health risks associated with smoking, the health and life insurance companies charge higher premiums from smokers than non-smokers. Therefore, the insurance companies, schools, and industrial companies perform test using blood cotinine measurement to determine whether the person is a smoker or non-smoker, as a serum sample is usally taken during a medical examination of application. So, there are needed to develop of sensitive and high-throughput tests for measuring cotinine.

In this reason, I hypothesized that using a high specific antibody is critical factor in developing sensitive enzyme immunoassay. In addition to this, I also hypothesized that anti-cotinine antibody could function as an alternative *in vivo* and *in vitro* carriers in complex with cotinine for its characteristics such as non-toxic, well-studied metabolism, and physiologically absent cellular receptors.

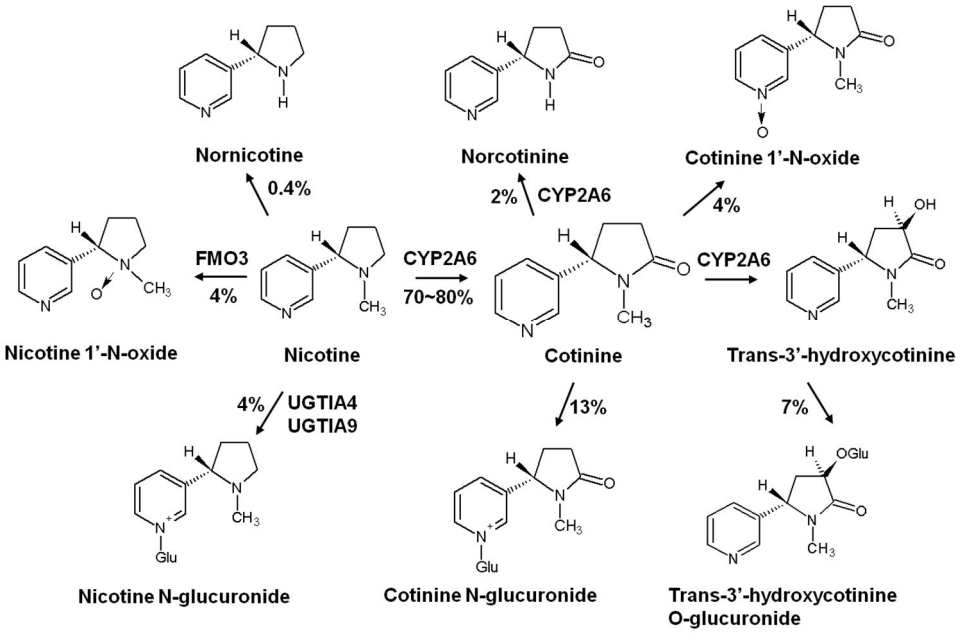

Figure 1. Nicotine and cotinine metabolism.

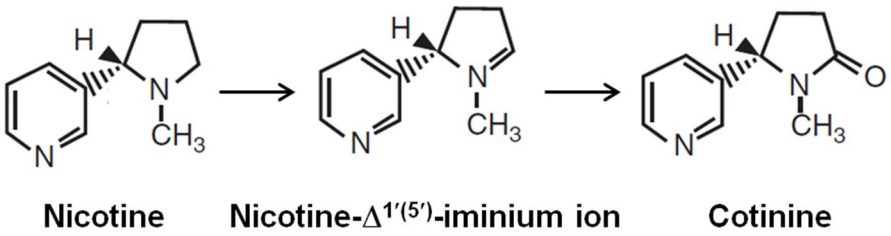

Figure 2. Conversion of nicotine to cotinine.

(Shigenaga *et al*., 1988)

Ⅱ. Monoclonal anti-cotinine antibody

Ⅱ-1. Phage display technology

Phage display technology was first introduced in 1985 by George Smith (Smith, 1985). Fragments of the EcoRI endonuclease, displayed as a polypeptide fusion (phenotype) to the gene 3 protein (g3p), were encoded on the DNA molecule (genotype) encapsulated within the phage particle. He has shown that phages could be used as a library of genetic information and used as an expression vector, capable of presenting a foreign amino acid sequence accessible to binding an antibody. The linkage of genotype to phenotype is the fundamental aspect of phage display.

Since then, a large number of phage displayed peptide and protein libraries have been constructed (Bass *et al.*, 1990; McCafferty *et al.*, 1990; Barbas *et al.*, 1991; Smith, 1991; Smith and Scott, 1993; Szardenings, 2003), leading to various techniques for screening such libraries. This technology has had a major influence on the work and discoveries done in the fields of immunology, cell biology, pharmacology and drug discovery. Phage display allows the presentation of large peptide and protein libraries on the surface of filamentous phage, which leads to the selection of peptides and proteins, including antibodies, with high affinity and specificity to almost any target. The technology involves the introduction of exogenous peptide sequences into a location in the genome of the phage capsid proteins. The encoded peptides are expressed or “displayed” on the phage surface as a fusion product with one of the phage coat proteins. This way, instead of having to genetically engineer different proteins or peptides one at a time and then

express, purify, and analyze each variant, phage display libraries containing up to 10^{10} variants can be constructed simultaneously. The main features of the phage display technology were the direct linkage to their own genome of peptide or protein for display, isolation of peptides or proteins against target molecules by specific selection process called 'bio-panning', and the significantly large sequence complexity of library, which increases high probability to isolate the most specific binder (Smothers *et al.*, 2002).

The strength of phage technology is its ability to identify interactive regions of proteins and other molecules without preexisting notions about the nature of the interaction. The past decade has seen considerable progress in the applications of phage display technology. Different bio-panning methods have allowed isolation and characterization of peptides binding to several molecules in vitro, in the context of living cells, in animals and in humans (Arap *et al.*, 2002).

Ⅱ-2. Antibody phage libraries

Antibody (scFv, Fab) repertoires have been generated using a variety of phage display formats. Antibody genes can be provided from immune donors, or synthetically in vitro. Lymphocytes are isolated from the spleen or bone marrow of an immunized animal, and genetic elements of variable regions of antibody are obtained by family-based oligonucleotides (Marks *et al.*, 1991). Construction of antibody libraries involves rearranging V_H and V_L gene segments in vitro and introducing artificial complementarity determining region (CDRs) of varying loop lengths using PCR and randomized oligonucleotide primers. These assembled gene repertoires were cloned into an

appropriate phagemid vector and transformed into E.coli bacteria. After transfected with helper phages, finally phages displaying antibody were obtained. Many secreted eukaryotic proteins such as antibodies require disulphide bonds for stability, and the oxidizing environment of the E. coli periplasm, where filamentous phage assembles, provides the appropriate conditions for antibody folding. The starting point is usually an antibody library comprising a population of, ideally, 10^9–10^{11} clones. One of the major advantages of phage display technology of antibody fragments compared with standard hybridoma technology is that the generation of specific scFv/Fab fragments to a particular antigen can be performed within a couple of weeks.

Ⅱ-3. Bio-panning

Bio-panning is an iterative process, where specific binder molecules are continuously enriched and multiplied from a pool of predominantly nonbinders until the specific binders finally become the majority population (Konthur *et al.*, 2005). For panning, antigens can be anchored to various types of solid supports, such as magnetic beads (Walter *et al.*, 2001), column matrix (Noppe *et al.*, 2009), nitrocellulose (Hawlisch *et al.*, 2001) or to a larger extent, plastic surfaces in the form of polystyrene tubes (Hust *et al.*, 2002), or 96 well polystyrene microtiter plates (Krebs *et al.*, 2001). The selection process is an affinity-based enrichment process and involves multiple rounds of selection. The antibody presenting phage particles are incubated with the immobilized antigens to allow interactions to occur. Next, nonbinders are removed from the selection matrix by washing off unbound phage particles. The bound phages are then used to infect Escherichia coli

and are subsequently re-amplified to be used in the following round. This selection cycle is normally repeated until a satisfactory enrichment is achieved. Normal panning protocols usually constitute between two and four rounds. Key stages in the selection procedure are panning, infection, propagation, colony picking, and ELISA evaluations. High-throughput approaches are required to circumvent the need for faster and more efficient screening protocols and to allow simultaneous selection and evaluation of enriched antibody phage libraries. Possible panning procedures compatible with automation involve immobilization of antigens to either 96 well microtiter plates (Krebs et al., 2001) or magnetic beads (Walter et al., 2001). The overall process from antibody phage library generation to antibody purification is shown in Fig. 3.

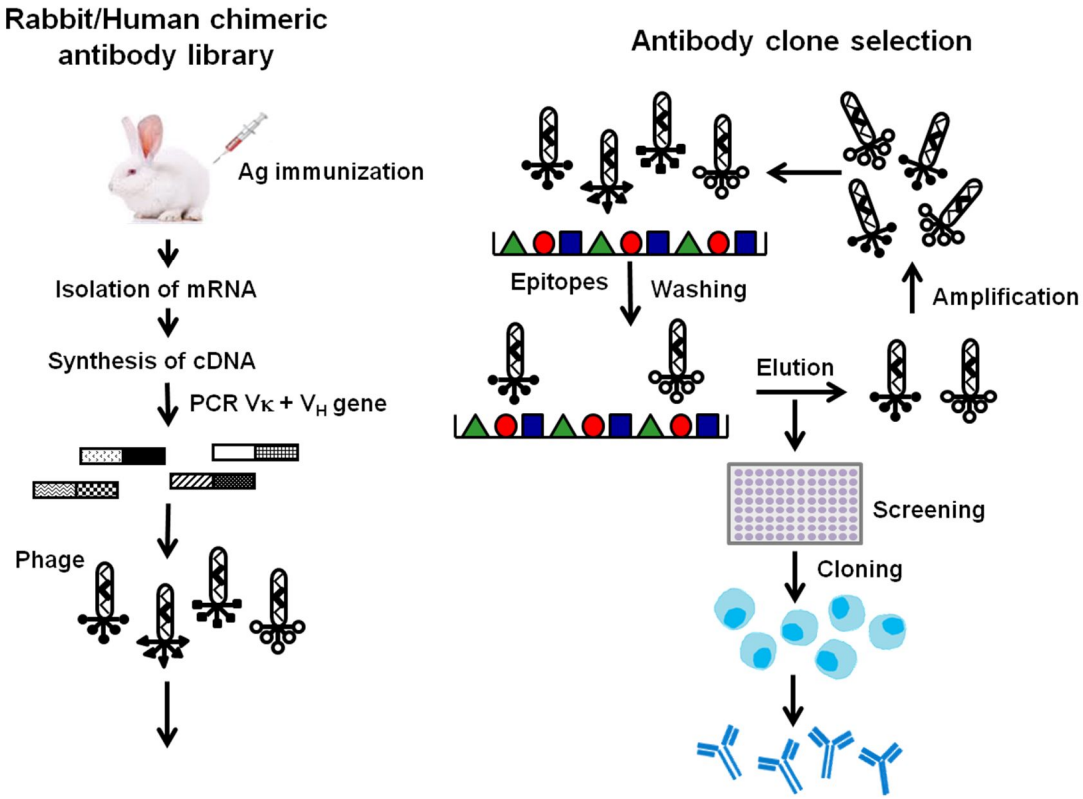

Figure 3. Overall process of antibody generation from construction of antibody phage library to selection of positive antibody clones.

After immunizing antigen to rabbit, total RNA was prepared from spleen and bone marrow followed by cDNA synthesis by reverse transcription. cDNA encoding for the heavy and the light variable regions of antibodies (V_H, V_L) are amplified from RNA by

PCR and assembled. The assembled genes are inserted into a phagemid vector with the gene encoding the pIII. The vector is introduced into E.coli. After rescue with helper phage, the random combinatorial library of antibodies is displayed on phage. This large antibody phage library containing millions of different ligands can be isolated by a series of recursive cycles of selection on antigen such as bio-panning, each of which involves bind, washing, elution, and amplification. After bio-panning, the resultant phage pool can be tested in an ELISA to evaluate the success of bio-panning and selected antibody phage clones are produced and purified as an antibody protein.

Ⅲ. A sensitive enzyme immunoassay for measuring cotinine in passive smokers

Ⅲ-1. Exposure to passive smoking

Passive smoking is a widespread source of nicotine exposure (Hammond, 1999); about 60% of the U.S. population is exposed to passive smoking. The amount of nicotine obtained from passive smoking depends on the concentration, duration, and frequency of exposure (Jaakkola and Jaakkola, 1997). Nicotine is released while cigarettes burn and is contained in expired air after puff inhalations, as roughly 82-92% of nicotine inhaled during active smoking is absorbed (Armitage *et al.*, 1975; Iwase *et al.*, 1991). In mainstream smoke-that is, what is taken in by the smoker-nicotine is contained in particles (composed of tar, water, and other nicotine-like alkaloids). In passive smoking, most of the nicotine leaves the particulate phase and becomes part of the gaseous or vapor phase (Heimke *et al.*, 1989; Nesmeianova *et al.*, 1991). Nicotine in passive smoking is breathed into the nose and throat and is inhaled into the lungs by nonsmokers. Nicotine is extremely soluble in water and is highly extracted from passive smoking within the respiratory tree (Iwase *et al.*, 1991).

According to the case study of risk of the non-smoker in Switzerland, nearly 92% of Swiss people were exposed to passive smoking. Particularly, 7% of them including workers of restaurants, coffees, bars, discotheques are exposed to more than 15-38 cig/day when nicotine and its biomarkers, salivary nicotine and cotinine was monitored.

With passive smoking exposure being pervasive and potentially containing high

concentrations of nicotine, passive smoking increases the risk of numerous diseases, including coronary heart diseases (Whincup *et al.*, 2004), chronic obstructive lung disease (Yin *et al.*, 2007), stroke (Iribarren *et al.*, 2004; He *et al.*, 2008) and peripheral arterial disease (He *et al.*, 2008). Passive smoking contains known carcinogens, such as polycyclic aromatic hydrocarbons and 4-aminobiphenyl, which react with DNA and proteins to form adducts (Tang *et al.*, 1999; Sexton *et al.*, 2004). These compounds have been associated with the development of cancer (Tang *et al.*, 2001; Perera *et al.*, 2002). Nonsmoking pregnant women passively exposed to tobacco smoke also have increased risk of giving birth to children with low birth weight (Hegaard *et al.*, 2006). And passive smoking is also a major cause of morbidity and mortality among children. Passive smoking increases the risk of sudden infant death syndrome (SIDS), otitis media, lower respiratory tract infections, and asthma (Cook and Strachan, 1999; Larsson *et al.*, 2001). Some of these effects of secondhand smoke in nonsmokers are comparable to the effects of smoking in smokers, even to the comparatively low doses of smoke (compared with smoking) that nonsmokers inhale when around secondhand smoke, perhaps because the effects of the toxins in the smoke saturate at relatively low exposures.

Ⅲ-2. Cotinine as a tobacco biomarker in passive smoking

The National Research Council has proposed criteria for a valid marker of passive smoking in the air as follows : The marker 1) should be unique or nearly unique for passive smoking so that other sources are minorr in comparison; 2) should be easily detectable; 3) should be emitted at similar rates for a variety of tobacco products; and 4)

should have a fairly constant ratio to other passive smoking components of interest under a range of environmental conditions encountered (National Research Council. Environmental tobacco smoke : measuring exposures and assessing health effects. Washington, DC : National Academy Press, 1986). Furthermore, the validity of a biomarker depends on the accuracy of the biologic fluid measurement in quantitating the intake of the marker chemical, which in turn may be influenced by individual differences in rates or patterns of metabolism or excretion, the presence of other sources (such as diet) of the chemical, and the sensitivity and specificity of the analytical methods used to measure the chemical. Measurement of cotinine in biologic fluids meets these criteria reasonably well. There is interindividual variability in any biologic measurements. While such variability may limit the value of prediction based on a measurement in an individual, variability is compensated for in studies of large numbers of subjects, as in epidemiologic studies. In support of this conclusion is the observation that cotinine levels in nonsmokers have positively correlated to the risks of some passive smoking-related health complications in children. Therefore, cotinine levels provide a valid and quantitative measure of average human passive smoking exposure over time. Cotinine is clearly the best available biomarker of passive smoking exposure at present.

Cotinine levels <10 ng/mL are considered to be consistent with no active smoking. Values of 10 ng/mL to 100 ng/mL are associated with light smoking or moderate passive exposure, and levels above 300 ng/mL are seen in heavy smokers - more than 20 cigarettes a day. In urine, values between 30 ng/mL to 100 ng/mL may be associated with light smoking or passive smoking, and levels in active smokers typically reach 500 ng/mL

or more. Nicotine is rapidly metabolized and has a short half-life, but cotinine is metabolized and eliminated at a much lower rate. Cotinine assays provide an objective quantitative measure that is more reliable than smoking histories or counting the number of cigarettes smoked per day.

Ⅲ-3. Enzyme immunoassay kits

In the majority of previous studies on passive smoking, the degree of exposure to tobacco smoke was determined based on answers to questionnaires due to a lack of standard high-throughput methods for determining the level of exposure to environmental tobacco smoke. Earlier methods for measuring serum cotinine levels included enzyme-linked immunosorbent assay (ELISA) (Gonzalez *et al.*, 1996), radioimmunoassay (Seccareccia, Zuccaro *et al.*, 2003), liquid chromatography (Machacek and Jiang, 1986), gas chromatography (Feyerabend and Russell, 1990), and high pressure liquid chromatography, alone or coupled with mass spectroscopy (Wong *et al.*, 1991; Ji *et al.*, 1999; Tuomi *et al.*, 1999). Unlike most other methods, ELISA is easy to design and standardize for high-throughput analyses. However, the lower limit of quantification (LLOQ) for cotinine is higher than passive smoking level with currently available ELISA kits because of using low affinity anti-cotinine antibody in ELISA kit. Unlike most other earlier methods including liquid chromatography, gas chromatography, and high pressure liquid chromatography, ELISA is easy to design and standardize for high-throughput analyses.

Table 1 present FDA approved commercialized ELISA kit and strips for measuring

cotinine in various biological samples. However, the cut-off for serum cotinine is >10 ng/mL with currently available ELISA kits. And this low sensitivity of these ELISA kits makes them unsuitable for detecting and categorizing passive exposure to smoke at levels that result in serum cotinine concentrations of 1 to 15 ng/mL typical to passive smokers (Seccareccia *et al.*, 2003; Whincup *et al.*, 2004). Therefore, methods with greater sensitivity are needed for high-throughput detection of passive smokers and quantification of their serum cotinine levels.

Here, I develop an ELISA for cotinine that has an LLOQ of 1 ng/mL and cut off of 5.1 ng/mL using selected a recombinant antibody to cotinine using a phage display of combinatorial antibody library and evaluated the assay in animals injected with nicotine and in human subjects exposed to tobacco smoke. This method was sufficiently sensitive for monitoring temporal changes in serum cotinine levels in rats injected with nicotine at doses similar to those present in individuals passively exposed to the smoke from one tenth of a cigarette.

Table 1. Defects of previous EIA kit for detecting passive smoking.

Name	Manufacturing	Detection limit	Cut-off value	Type
Omni-SAL Saliva kit Omni urine kit	Cozart Bioscience Ltd	1 ng/mL 1.2 ng/mL	50 ng/mL 500 ng/mL	Saliva Urine
Cotinine micro-plate EIA kit	STC-technologies,Inc	10 ng/mL	50 ng/mL	Saliva
Auto-Lyte Cotinine EIA Cotinine micro-plate EIA	Orasure	1 ng/mL 10 ng/mL	500 ng/mL 25 ng/mL	Urine Serum
dBest One Step COT Test Kit	AmeriTek	5 ng/mL	500 ng/mL	Urine
NicAlert	NYMOX	10 ng/mL	50 ng/mL	Urine
AccuSign Nicotine	PBM		500 ng/mL	Urine
NicCheck 1 strips				Urine

Ⅳ. *In vivo* carrier for cotinine conjugated molecule

Ⅳ-1. Effects of PEGylation as drug delivery system

The biotechnology revolution has produced novel peptides and polypeptides that have become important new drugs. It was estimated that in the year 2000, More than 80 polypeptide drugs are marketed in the United States, and 350 more are undergoing clinical trials. These advances due to: 1) discovery of novel peptides and proteins, 2) a better understanding of the mechanism of action in vivo, 3) improvements in expression or synthesis of proteins and peptides that closely resemble fully human proteins and peptides, and 4) improvements in formulation or molecule-altering technologies that have the ability to deliver polypeptides in vivo with improved pharmacokinetic and pharmacodynamic properties. Despite these tremendous advances, peptide and polypeptide drugs possess several shortcomings that limit their usefulness. Since the limitations encountered in the use of small drugs are their susceptibility to destruction by proteolytic enzymes low solubility and immunigenisity, short circulating half-life, rapid kidney clearance due to their small size, they have extremely short elimination half-lives *in vivo* (Roberts *et al.*, 2002). Several strategies have emerged as ways to improve the pharmacokinetic and pharmacodynamic properties of biopharmaceuticals, including: manipulation of amino acid sequence to decrease immunogenicity and proteolytic cleavage, fusion or conjugation to immunoglobulins and serum proteins, such as albumin, incorporation into drug delivery vehicles for protection and slow release, and conjugating to natural or synthetic polymers (Cohen *et al.*, 1991; Syed *et al.*, 1997; Mateo,

Lombardero *et al.*, 2000; Walsh, 2000).

Pegylation is mostly preferable method that overcomes deficiencies of peptide and polypeptide drugs. PEGylation defines the modification of a polypeptide, peptide or non-peptide molecule by the linking of one or more polyethylene glycol (PEG) chains. The FDA has approved PEG for use as a vehicle. This polymer shows little toxicity, and low immunogenicity, and high soluble in water (Richter and Akerblom, 1983). Therefore, PEGylated drugs have several advantages: a prolonged residence in body, a inhibited their renal clearance (Pasut and Veronese, 2011), a decreased degradation by metabolic enzymes and a reduction or elimination of protein immunogenicity.

Thanks to these favorable properties, PEGylation now plays an important role in drug delivery, enhancing the potentials of peptides and proteins as therapeutic agents. However, PEGylation is encountered some limitations: 1) polydipersivity, 2) low loading of PEG, and 3) difficulty of process development. 1, 2) Polydisperse issue and low lading of PEG is more critical for dealing with small peptide because their low molecular weight molecule is more affected to size, which leads to a molecular heterogenesity of drug conjugates and insufficient stability, respectively, and which might have different biological properties in body half-life. To overcome these problems, construction of dendrimeric PEG structures and monodisperse PEG is suggested but the synthesis of PEG dendrons and high molecular weight monodisperse PEG are difficult to production. 3) In addition, the process of PEGylation is time-consuming and inconvenient as it requires a secondary purification of the derivatized polypeptide. And in some cases, special linker between PEG and drug might be desirable for a drug to be released from its PEG polymer

when it reaches a target site to improve its action. Therefore, PEGylation needed special chemistry or complex process.

Ⅳ-2. Cotinine-peptide conjugate and anti-cotinine antibody complex as a novel drug delivery system

As mentioned above, PEGylation can inhibit their renal clearance, but usually polydiperse and requires time-consuming, peptide-specific optimization. I hypothesized that an anti-hapten antibody could function as an alternative peptide carrier in complex with its corresponding hapten. For this purpose, the hapten must be non-toxic and physiologically absent and inert in animals and humans. Additionally, its metabolism must be well characterized. As a major metabolite of nicotine to which humans have long been exposed, cotinine is an appropriate hapten for this application. Cotinine is a relatively safe molecule with an LD_{50} of 2-4 g/kg in mice (Riah *et al.*, 1999), and doses up to 1.8 g per day during a four-day period did not induce detectable negative effects and were well tolerated in humans4. Its metabolism in mammals is well known, with a serum half-life of approximately 20 h. In human cotinine is absent physiologically and up to 160 mg cotinine intake for three consecutive days did not induce any physiological and behavioral effect (Hatsukami *et al.*, 1997) (Fig. 4).

The peptide Trp-Lys-Tyr-Met-Val-D-Met-CONH2 (WKYMVm-NH_2) is effective in treating experimental sepsis. However, injection of large amounts of the peptide (4 mg/kg twice per day for 2 days) was required, which might be due to its short half-life (Kim *et al.*, 2010). In this study, I conjugated the WKYMVm-NH_2 peptide to cotinine and then tested whether the conjugated peptide within an anti-cotinine rabbit/human chimeric antibody complex would retain its characteristics and exhibit therapeutic efficacy at lower doses.

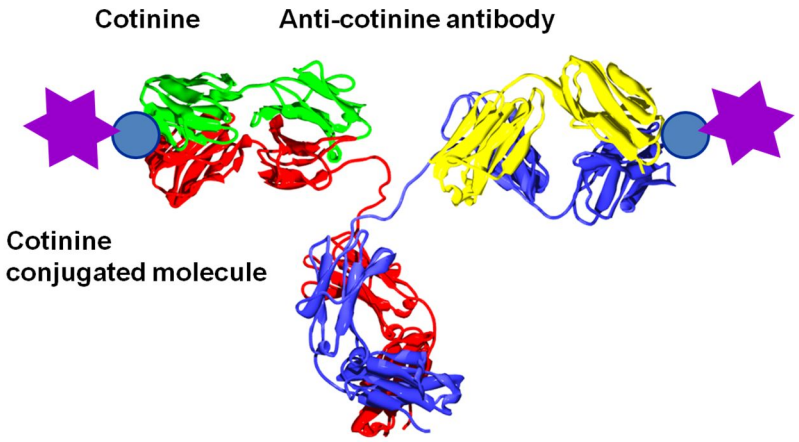

Figure 4. cotinine, cotinine conjugated molecule and anti-cotinine antibody complex platform.

(Antibody structure was from "http://proteopedia.org/wiki/index.php/Antibody")

Ⅳ-3. WKYMVm-NH_2 and its therapeutic efficacy in sepsis

Trp-Lys-Tyr-Met-Val-d-Met (WKYMVm) is an analogue of WKYMVM which was originally identified from a combinatorial library of peptides by functional screening based on stimulation of phosphoinositide (PI) hydrolysis in a human B myeloma cell line (U266) (Baek *et al.*, 1996; Seo *et al.*, 1997). WKYMVm-NH_2 was developed by substituting the l-methionine at the C-terminus of WKYMVM with a d-methionine and by further modifying the COOH residue with a NH_2 residue. These modifications markedly improved the biological activities of the peptide (Seo e*t al.*, 1997) (Table 2).

WKYMVm-NH_2 was known to agonist of members of the formyl peptide receptor (FPR) family (mFPR1 and mFPR2 in mice, and FPR1, FPR2, and FPR3 in humans), G protein-coupled seven transmembrane receptors, to exert its biological activities (Le *et al.*, 1999; Dahlgren *et al.*, 2000; Christophe *et al.*, 2001). WKYMVm-NH_2 was shown to stimulate phagocyte including human neutrophils and monocytes, and enhances the bactericidal activity via superoxide generation, chemotactic migration and survival by blocking apoptosis (Bae *et al.*, 1999; Bae *et al.*, 1999; Bae *et al.*, 2000; Bae *et al.*, 2002). Recently, human dendritic cells, the mouse DC cell line, DC2.4 and mouse bone marrow-derived DCs (mBmDCs) have been shown to express some of FPR family (Yang *et al.*, 2002; Lee *et al.*, 2004). Through the interaction with the receptors, WKYMVm-NH_2 stimulates multiple signaling cascades and modulates several functions in human monocyte-derived cells including dendritic cells and the DC2.4 cells.

Sepsis occurs when host immune defenses fail to combat invading microbes. In the United States, sepsis is leading cause of death in critically ill patients and the incidence of

severe sepsis develops in 750,000 people annually, and more than 210,000 of them die. After numerous unsuccessful trials of anti inflammatory agents in patients with sepsis, investigators doubted that mortality could be decreased. Sepsis-induced mortality is accompanied by an inability to regulate the inflammatory response because of substantial impairment of the innate immune system during early sepsis (i.e., during the first 6 h). In addition, excessive lymphocyte apoptosis occurs during sepsis, resulting in the clinical signs of multiorgan failure. Moreover, cytokine levels are markedly altered during sepsis; in particular, the levels of such proinflammatory cytokines as TNF-a and IL-1b are greatly increased.

Administration of WKYMVm-NH_2 inhibited the production of proinflammatory cytokines and enhanced IL-17 production. And in vitro stimulation of low or high doses of LPS to inflammatory cells significantly inhibited proinflammatory cytokine production when cells were coincubated with IL-17. Therefore these data suggest that anti-inflammatory effect of WKYMVm-NH_2 in the sepsis model can be partly explained by the downregulation of proinflammatory cytokine production by IL-17 augmented by mFPR activation (Kim *et al.*, 2010).

Table 2. Effect of the peptides modified from MKYMPM-NH_2, and WKYMVM-NH_2, on the PI hydrolysis in U266 cells.

Sequence	EC_{50} (μM)	Sequence	EC_{50} (μM)
MKYMPM-NH_2	1.2 ± 0.24	MKYMPH-NH_2	1.2 ± 0.24
CKYMPM-NH_2	72 ± 18	mKYMPM-NH_2	3.3 ± 0.12
MGYMPM-NH_2	>100	MkYMPM-NH_2	13 ± 4.5
MKGMPM-NH_2	inactive	MKyMPM-NH_2	62 ± 15
MKYGPM-NH_2	>100	MKYmPM-NH_2	>100
MKYMGM-NH_2	inactive	MKYMpM-NH_2	29 ± 7.4
MKYMPG-NH_2	inactive	MKYMPm-NH_2	0.031 ± 0.0067
		Mkympm-NH_2	Inactive
KYMPM-NH_2	50 ± 12		
YMPM-NH_2	>100	WKYMVM-NH_2	0.061 ± 0.012
KYMP-NH_2	inactive	wKYMVM-NH_2	8.2 ± 2.5
MKYM-NH_2	33 ± 8.5	WkYMVM-NH_2	10 ± 3.5
MKYMP-NH_2	Inactive	WKyMVM-NH_2	12 ± 4.5
		WKYmVM-NH_2	0.13 ± 0.072
		WKYMvM-NH_2	0.063 ± 0.0095
		WKYMVm-NH_2	0.00051 ± 0.0095
		wkymvm-NH_2	inactive

Ⅴ. *In vitro* carrier for cotinine conjugated molecule

Ⅴ-1. Aptamer and noble affinity unit for biological assay using aptamer

Aptamers are synthetic, relatively short (e.g., 20-80 bases) RNA or ssDNA oligonucleotides that can fold into unique, three-dimensional shapes. Aptamers can bind to targets with high affinity and specificity and were first described as affinity molecules for protein binding in 1990 (D'Angelo *et al.*, 1990; Ellington and Szostak, 1990; Tuerk and Gold, 1990). Following the development of the SELEX (systematic evolution of ligands by exponential enrichment) method, in vitro selection and amplification techniques became more efficient and easier to perform (Oguro *et al.*, 2003; Miyakawa *et al.*, 2006; Ohuchi *et al.*, 2006). Aptamers can form stable and specific complexes with a wide variety of targets, including small low molecular compounds such as amino acids (Jellinek *et al.*, 1993; Williams *et al.*, 1996; Proske *et al.*, 2002) and complex protein targets such as cell membrane proteins (Ulrich *et al.*, 1998; Homann and Goringer, 1999; Blank *et al.*, 2001; Ulrich *et al.*, 2002; Guo *et al.*, 2006).

Aptamers have been used in various methods in which antibodies have been commonly used, such as in enzyme immunoassays, immunoprecipitation analyses, flow cytometric analyses (Ireson and Kelland, 2006; Ferreira *et al.*, 2008; Sakai *et al.*, 2008), protein microarrays (Chen *et al.*, 2008), magnetic-separation assays (Gao *et al.*, 2007), lateral flow assays (Liu *et al.*, 2007; Shaikh *et al.*, 2007), and biosensor methods (Backmann *et al.*, 2005; Borisov and Wolfbeis, 2008). Aptamers can be either conjugated to beads or surfaces, or labeled with enzymes or fluorescent dyes for use in such

applications. However, the development of specific conditions for conjugation or labeling is a time-consuming process. The labeling of aptamers with biotin to produce complexes with avidin in various forms has been commonly employed (Murphy *et al.*, 2003; Baldrich *et al.*, 2005; Li *et al.*, 2009; Tanaka *et al.*, 2009). Additionally, labeling aptamers with digoxigenin to produce complexes with anti-digoxigenin antibodies also has been used (Ramos *et al.*).

In this report, I introduce cotinine-conjugated aptamer/anti-cotinine antibody complexes as an alternative and complementary platform for the use of aptamers in biological assays. I utilized two well-known aptamers: AS1411 (Bates *et al.*, 1999; Dapic *et al.*, 2002; Dapic *et al.*, 2003) and pegaptanib (Ruckman *et al.*, 1998; Ng and Adamis, 2006). Cotinine-conjugated AS1411/anti-cotinine antibody complexes were successfully applied to immunoblot, immunoprecipitation, and flow cytometric analyses, and cotinine-conjugated pegaptanib/anti-cotinine antibody complexes were successfully used in enzyme immunoassays.

Ⅴ-2. AS1411 and pegaptanib

AS1411 is the 26-oligomer DNA aptamer and first aptamer to enter clinical oncology trials. It has shown both promising antitumor activity and a lack of serious systemic toxicity in a phase I clinical trial. Multi-institutional phase II clinical trials of AS1411 in refractory or relapsed acute myeloid leukemia (AML) (clinicaltrials.gov identifier NCT00512083) and in renal cancer (NCT00740441) are now under way. AS1411 is target nucleolin on various types of tumor cells (Bates *et al.*, 1999; Otake *et al.*, 2005;

Soundararajan *et al.*, 2008). Nucleolin is expressed at high levels on the surface of cancer cells and has a remarkably multi-function in intracellular. AS1411 uptake would be more extensive in tumor cells than in normal cells because normal cells lack or have lower levels of the nucleolin in the plasma membrane. Nucleolin has been shown to bind G-quadruplex-forming DNA sequences (Dapic *et al.*, 2003). Because AS1411 forms a stable G-quadruplex structure, this probably contributes to the high affinity and specific binding of the DNA aptamer to nucleolin. AS1411 involve in mediating a wide range of pathways, including endocytosis, cellular adhesion, signal transduction, and as a receptor for various pathogens. Intracelluar nucleolin interact with tumor-associated angiogenic endothelial cells and hundreds of other molecules (proteins, nucleic acids, peptides, nucleotides and sugars) and has been reported as a regulator of a similarly high number of cellular processes, including ribosome biogenesis, DNA replication, transcription, translation, chromatin remodeling, apoptosis, cytokinesis, protein trafficking and telomere maintenance. AS1411 uptake followed by binding to nucleolin in tumor cell surface contribute to the antiproliferative effects to tumor cell including which are binding to nuclear factor-κB (NF-κB) essential modulator and cytoplasmic nucleolin to Bcl-2 mRNA (anti-apoptotic Bcl-2 protein) causing to inhibition the activation of NF-κB and expression of anti-apoptotic Bcl-2 protein, respectively. AS1411 also can increase BMP-2 mRNA stability and protein levels (Fig. 5).

Pegaptanib is the 28-oligomer RNA aptamer nuclease-resistant aptamer that binds with high affinity to the isoform of vascular endothelial growth factor (VEGF), which is a key regulator of both physiological and pathological angiogenesis (Fig. 6). Pegaptanib have

high binding affinity for VEGF165 of approximately 200 pM. Pegaptanib is approved for the treatment of age-related macular degeneration (AMD) and also is undergoing clinical trials as a treatment for other ocular vascular diseases, including diabetic macular edema (DME). Pegaptanib is highly modified to inhibit proteolysis and degradation. Endonuclease resistance was enhanced through the incorporation of 2′-fluoropyrimidines, 2′-O-methyl substitution of the majority of the purines and the addition of a 3′-3′-linked deoxythymidine terminal cap. A 40 kDa polyethylene glycol moiety was added to the 5′ terminus to prolong the duration of tissue exposure (Ruckman *et al.*, 1998).

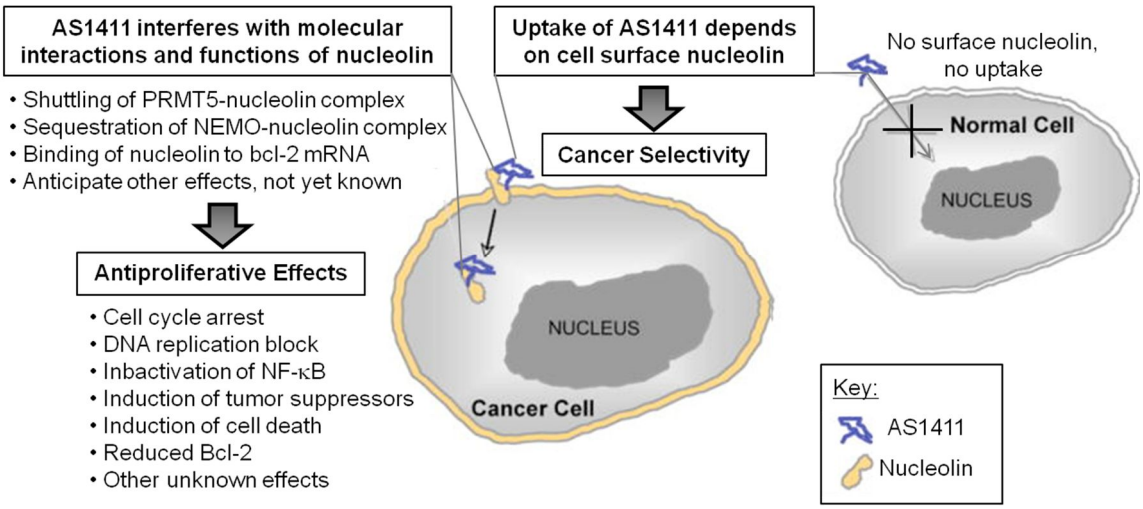

Figure 5. Proposed model for AS1411 mechanism of action.

The cellular uptake of AS1411 is dependent upon cell surface nucleolin. Because cancer cells have high levels of surface nucleolin compared to normal cells, this would explain the preferential uptake and activity of AS1411 in malignant cells. AS1411 causes pleiotropic antiproliferative effects because it interferes with some of the normal functions of nucleolin, which plays a role in many cancer-associated pathways. Some of the nucleolin complexes that are affected by AS1411 have already been identified, including those with PRMT5, NEMO and Bcl-2 mRNA (Bates JP *et al*., 2009).

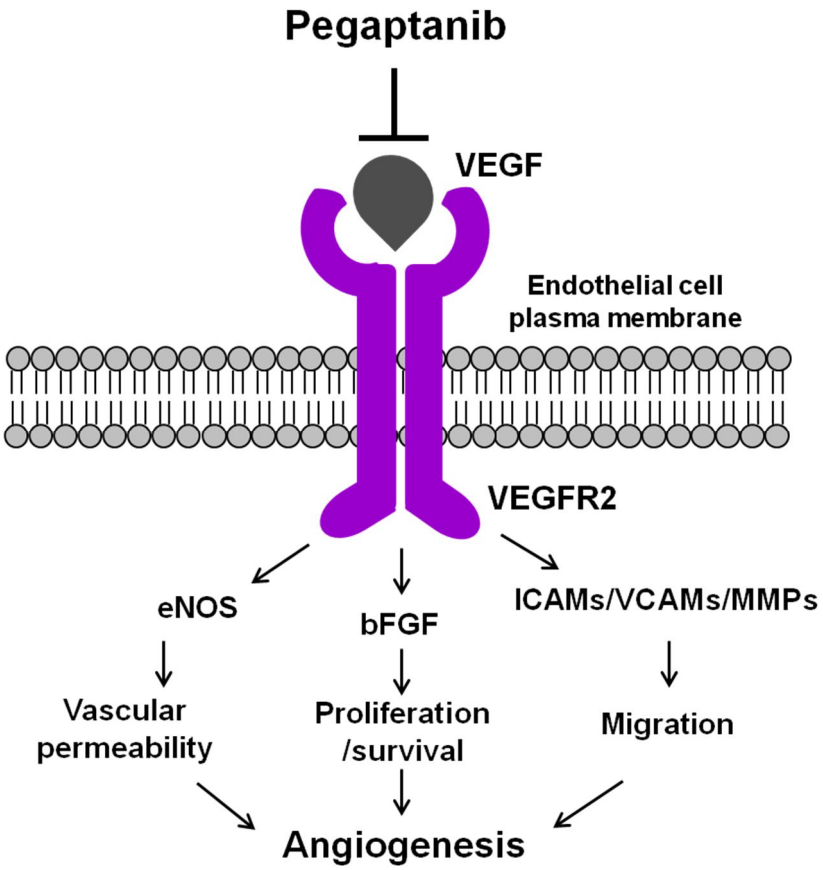

Figure 6. Proposed model for pegaptanib mechanism of action.

(Ruckman *et al.*, 1998)

Materials and Methods

Generation of anti-cotinine scFv antibodies

Construction of phage display scFv library

Male New Zealand white rabbit was immunized and then boosted 7 times, alternately with 50 μg of cotinine-keyhole limpet hemocyanin or cotinine-ovalbumin conjugate (Abiox, Lake Oswego, OR) emulsified in the RIBI MPL-TDM-CWS adjuvant (Sigma, St. Louis, Mo) mixtures at 3-week intervals. Total RNA was isolated from the spleen and bone marrow of the rabbit using the acid guanidinium thiocynate-phenol-chloroform extraction method (Chomczynski and Sacchi, 1987). First-strand complementary cDNA (cDNA) was synthesized using oligo-dT primers and superScript^{TM} III First-Strand Synthesis System (Invitrogen, Carlsbad, CA). First round PCR was performed with 10 primer combinations for amplification of rabbit V_L (9 x V_κ and 1 x V_λ) coding sequences and 4 combinations for the amplification of rabbit V_H coding sequences (Fig. 7) using Expand High Fidelity PCR System (Roche Molecular Systems, Pleasanton, CA). Each PCR reaction was performed in a 100 μL mixture composed of 500 ng of cDNA, 60 pmol of each primer, 10 μL of 10x reaction buffer, 200 μM of dNTPs (Promega, Madison, WI), 0.5 μL of Taq DNA polymerase. The PCR reactions were carried out under the following conditions: 30 cycles of 15 sec at 94℃, 30 sec at 56℃, and 90 sec at 72℃, followed by a final extension for 10 min at 72℃. In second round PCR, the first round V_L products

were randomly joined with the first round V_H products by overlap extension PCR (Fig. 8). Each PCR reaction was performed in a 100 μL mixture composed of 100 ng of first round PCR products, 60 pmol of each primer, 10 μL of 10x reaction buffer, 200 μM of dNTPs, 0.5 μL of Taq DNA polymerase. The PCR reactions were carried out 20 cycles under the same conditions with first round PCR. The primers used in PCRs were presented in Table 3. The scFv products and pComb3x vector were digested with *Sfi* I restriction enzyme (32 units per ug of scFv products and 6 units per μg of vector) (Roche Melocular Systems) by incubating for 12 h at 50℃. 700 ng of the *Sfi* I-digested scFv products were ligated with 1400 ng of the pComb3x vector using T4 DNA ligase (Invitrogen) by incubating for 12 h at 16℃. After ethanol precipitation overnight at -80℃, 20 μL of total ligated library sample was transformed into 300 μL of ER2738 electrocompetent cells by electroporation with a 0.2 cm cuvette and Gene Pulser (Bio-Rad Laboratories, Hercules, CA) at a condition of 2.5 kV, 25 μF, and 200 Ω. The cells were resuspended with 5 mL of SB medium and incubated for 1 h at 37℃ while shaking at 250 rpm. 10 mL of prewarmed SB medium and 3 μL of 100 mg/mL carbenicillin were added to the culture. The library size was determined by plating 0.1 μL, 1 μL and 10 μL of the culture on LB plate containing 50 μg/mL of carbenicillin. The culture was shook for 1 h at 250 rpm and 37℃. 4.5 μL of 100 mg/mL carbenicillin was added to the culture and shook for an additional hour. The culture was added with 2 mL of VCSM13 helper phage, 183 mL of prewarmed SB and 92.5 μL of 100 mg/mL carbenicillin and shook for 2 h at 250 rpm and 37℃. 280 μL of 50 mg/mL kanamycin was added to the culture and the culture was shaking

overnight at 300 rpm and 37℃. The next day, the culture was centrifuged at 3000g for 15 min at 4℃. The bacterial pellet was saved for phagemid DNA preparations and the supernatant was transferred to clean 500 mL centrifuge bottle. After that, 8 g of polyethylene glycol-8000 (PEG-8000) and 6 g of NaCl were added. After stored on ice for 30 min, the supernatant was spun at 15000g for 15 min and 4℃. The supernatant was discarded and the phage pellet was resuspended in tris-buffered saline (TBS) containing 1% BSA.

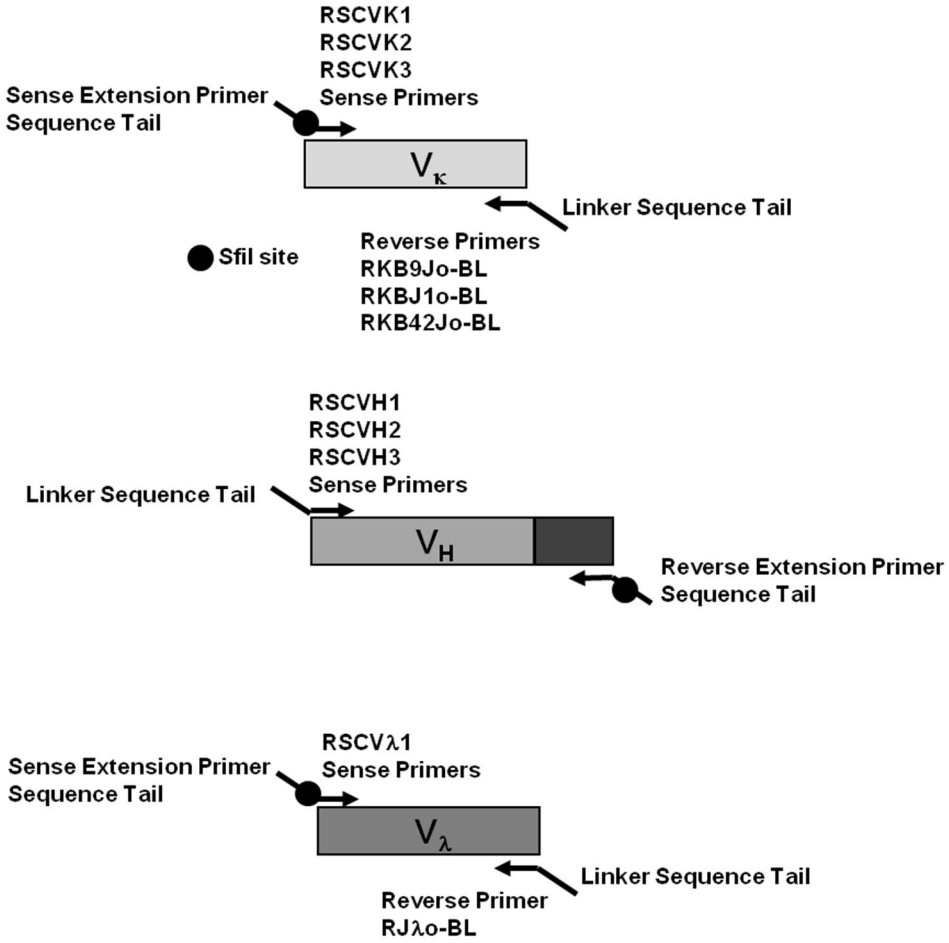

Figure 7. The amplification of rabbit V_κ, V_λ, and V_H sequences for the construction of scFv libraries (long linker).

Each sense primer is combined with each reverse primer to amplify rabbit V_κ, V_λ, and V_H gene segments from cDNA. The sense primers of V_κ and V_λ have a 5′ sequence tail that contains a *Sfi* I site and is recognized by the sense extension primer used in the

second round PCR. Each reverse primer of V_κ and V_λ has a linker sequence tail that is used in the overlap extension. The sense primers of V_H have a sequence tail corresponding to the linker sequence that is used in the overlap extension PCR and the reverse primer of V_H has a sequence tail containing a *Sfi* I site; this tail is recognized by the reverse extension primer used in the second round PCR. (Barbas CF, 3rd, Burton DR, Scott JK, Silverman GJ. Phage Display-A Laboratory Manual. New York: Cold Spring Harbor Press; 2001. p. 9.82-9.84.)

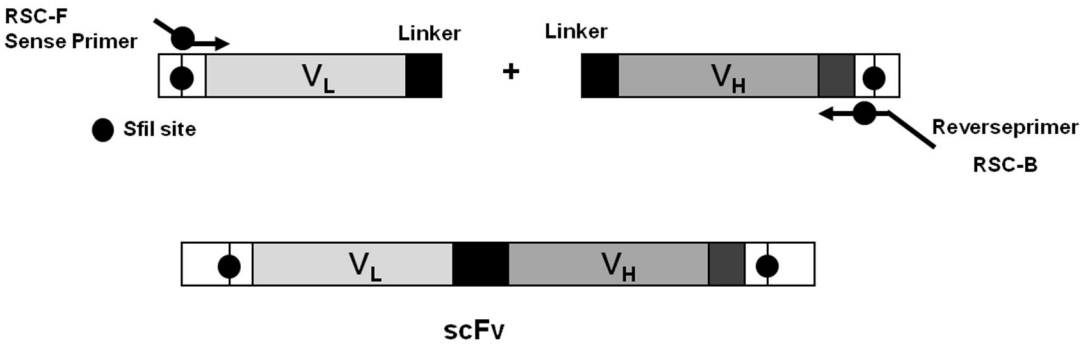

Figure 8. The overlap extension PCR to combine the rabbit V_L and V_H fragments for the construction of scFv libraries (long linker).

The sense and reverse extension primers used in this second round of PCR (RSC-F and RSC-B) recognize the sequence tails that were generated in the first round of PCR. (Barbas CF, 3rd, Burton DR, Scott JK, Silverman GJ. Phage Display-A Laboratory Manual. New York: Cold Spring Harbor Press; 2001. p. 9.85.)

Table 3. Primers for rabbit scFv libraries.

V_κ 5′ sense primers (5′ → 3′)	
RSCVK1	GGG CCC AGG CGG CCC AGC TCG TGM TGA CCC AGA CTC CA
RSCVK2	GGG CCC AGG CGG CCG AGC TCG ATM TGA CCC AGA CTC CA
RSCVK3	GGG CCC AGG CGG CCG AGC TCG TGA TGA CCC AGA CTC AA
V_κ 3′ reverse primers (5′ → 3′)	
RKB9Jo-BL	GGA AGA TCT AGA GGA ACC ACC TTT GAT TTC CACC ATT GGT GCC
RKBJ1o-BL	GGA AGA TCT AGA GGA ACC ACC TAG GAT CTC CAG CTC GGT CCC
RKB42Jo-BL	GGA AGA TCT AGA GGA ACC ACC TTT GAC SAC CAC CTC GGT CCC
V_λ 5′ sense primers (5′ → 3′)	
RSCλ1	GGC CCC AGG CGG CCG AGC AGC TCG TGA CTC AGT CCT C
V_λ 3′ sense primers (5′ → 3′)	
RJλo-BL	GGA AGA TCT AGA GGA ACC ACC CCC ACC ACC GCC CGA GCC ACC GCC ACC AGA GGA GCC TGT GAC GGT CAG CTG GGT CCC
V_H 5′ sense primers (5′ → 3′)	
RSCVH1	GGT GGT TCC TCT AGA TCT TCC CAG TCG GTG GAG GAG TCC RGG
RSCVH2	GGT GGT TCC TCT AGA TCT TCT CAG TCG GTG AAG GAG TCC GAG
RSCVH3	GGT GGT TCC TCT AGA TCT TCC CAG TCG YTG GAG GAG TCC GGG
RSCVH4	GGT GGT TCC TCT AGA TCT TGG CAG SAG CAG CTG RTG GAG TCC GG
V_H 3′ reverse primers (5′ → 3′)	
RSCG-B	CCT GGC CGG CCT GGC CAC TAG TGA CRG AYG GAG CCT TAG GTT GCC C
Primers for scFv overlap assembly	
RSC-F (sense)	GAG GAG GAG GAG GAG GAG GCG GGG CCC AGG CGG CCG AGC TC
RSC-B (reverse)	GAG GAG GAG GAG GAG GAG CCT GGC CGG CCT GGC CGG CCT GGC CAC TAG TG

Preparation of electrocompetent E.coli

The single E.coli colony from a glycerol stock that has been freshly streaked onto an agar plate was incubated to 15 mL of pre-warmed (37℃) SB in a 50 mL polypropylene tube and grew overnight at 250 rpm and 37℃. The next day, 2.5 mL of the culture was diluted into a 2 liter flask with 500 mL of SB, 10 mL of 20% (w/v) glucose, and 5 mL of 1 M $MgCl_2$ and shook at 250 rpm and 37℃ until the OD at 600 nm is about 0.8~0.9. After the proper OD is reached, the flask cultures were poured into a prechilled 500 mL centrifuge bottle and spun at 3000g for 20 min at 4℃. The supernatant was poured off and the pellet was resuspended in 300 mL of pre-chilled 10% (v/v) glycerol. The resuspended pellet was spun as before. After 3 times of the pellet washing with glycerol, the pellet was resuspended in the remaining volume and stored at -80℃.

Preparation of helper phage

10 μL of ER2738 was inoculated in 10 mL of SB medium and shook at 250 rpm for 1 h at 37℃. A single VCSM13 plaque from a freshly prepared plate was transferred to the culture using a pipet tip. The infected 10 mL culture was transferred to 2 liter Erlenmeyer flask containing 500 mL of prewarmed (37℃) SB containing kanamycin to a final concentration of 70 μg/mL, and was shaken overnight at 250 rpm and 37℃. The next day, the culture was spun at 2500g for 15 min and the supernatants were incubated in a water bath at 70℃ for 20 min. After spun at 2500g again for 15 min, the supernatants were transferred to fresh 50 mL polypropylene tubes and stored at 4℃.

Bio-panning on an immobilized antigen

To enrich specific binders, 5 rounds of bio-panning were performed as follows. Cotinine-bovine serum albumin (BSA) conjugate was dissolved (10 μg/mL) in PBS (137 mmol/L sodium chloride, 10 mmol/L phosphate, 2.7 mmol/L potassium chloride, pH 7.4), and 20 μL aliquots of this solution were added to each well of 96-well half-area microtiter plates (Corning Costar Corp., Cambridge, MA). After overnight incubation at 4°C, the wells were washed with PBS, 150 μL of 3% BSA in PBS was added to each well, and the plates were incubated for 1 h at 37°C. The wells were then washed with PBS and incubated with 50 μL of the phage library for 2 h at 37°C. The plates were washed with 0.05% Tween 20 in PBS (v/v) (PBST), once for the first round of biopanning, 3 times for the second and third rounds, and five times for the remaining two rounds, to remove unbound phage. The phage bound to the cotinine was eluted by adding 100 μg of cotinine dissolved in 50 μL of PBS to each well and incubating the plates for 30 min at 37°C. Eluted phages were used to infect ER2738 and the phagemid was rescued with VCSM13 helper phage for overnight amplification. Next day, phage was prepared by adding PEG-8000 and NaCl as described above. Also, the input and output phage titers were determined by plating the phage infected cultures on LB plate containing 50 μg/mL of carbenicillin.

Selection of clones by phage ELISA

To identify binding scFv from the individual clones selected for further analysis, an ELISA using phage displayed scFv was performed against cotinine-BSA. Microtiter

plates coated with cotinine-BSA were blocked for 1 h at 37℃ using 3% BSA in PBS. Then phage supernatants were equally mixed with 6% BSA in PBS and incubated for 1 hour at 37 ℃. After washing with 0.05% PBST, plates were incubated with an HRP-conjugated anti-M13 antibody (1:5,000 dilution; Pierce Chemical Co., Rockford, Ill). 2, 2'-azino-bis (3-ethylbenzothiazoline-6-sulphonic acid (ABTS) substrate solution (Amresco, Solon, OH) was used for the coloring reaction.

Sub-cloning into scFv-Fc and expression of scFv-Fc antibody

For production of the scFv-hinge-C_{H2}–C_{H3} (scFv–Fc), human IgG1 hinge-C_{H2}–C_{H3} region was amplified from a human bone marrow cDNA library (Clontech Laboratories, Inc., Palo Alto, CA) using 5' (GAGCCCAAATCTTGTGACAAAACTCAC) and 3' primers (GGATCCTCATTTACCCGGGGACAGGGAG). Overlap extension PCR was performed using 5' (GGGCCCAGGCGGCCGAGCTCGATCTGACCCAGACTCCA) and 3' primers (ACTCGAGCGTCATTTACCCGGGGACAGGAA), to generate a gene encoding the scFv–Fc. The gene was subcloned into the pCEP4 expression vector (Invitrogen) after digestion with *Xho* I (New England Biolabs, Beverly, MA) and *Sfi* I (New England Biolabs). For overexpression of the protein, HEK 293F cells (Invitrogen) were transfected with the pCEP4 vector encoding scFv–Fc and cultured in FreeStyle™ 293 expression medium (Invitrogen) containing 10 kIU/L penicillin and 100 mg/L streptomycin. The overexpressed scFv–Fc fusion protein was purified by protein A gel affinity chromatography in accordance with the manufacturer's instructions (Repligen Corp., Cambridge, MA).

Sub-cloning into IgG and expression of IgG antibody

The V_H and V_L were amplified from scFv–Fc gene using (ATCCTGTTCCTGGTGGCCACCGCCACCGGCCAGTCGGTGAAGGAGTCC) and (ATCCTGTTCCTGGTGGCCACCGCCACCGGCGAGCTCGATCTGACCCAG) as 5' primers and (TGAAGAGATGGTGACCAGGGTGCC) and (TAGGATCTCCAGCTCGGTCCCTCC) as 3' primers. Human IgG1 constant region (CH_1–CH_3) and human light chain constant region (C_κ) were amplified from a human bone marrow cDNA library (Clontech Laboratories, Palo Alto, CA) using (GTCACCATCTCTTCAGCCTCCACCAAGGGC) and (GAGCTCGGATCCCTTGCCGGCCGT) as 5' primers and (GAGCTGGAGATCCTACGGACCGTGGCCGCC) and (GCAAGCTCTAGACTAGCACTCGCC) as 3' primers containing annealing sites with V_H and V_L. Overlap extension PCR was performed using (ACATCGGCTAGCCGCCACCATGGGCTGGTCCTGCATCATCCTGTTCCTG) and (ACTTAAGCTTGCGCCACCATGGGCTGGTCCTGCATCATCCTGTTCCTG) as 5' primers and (GAGCTCGGATCCCTTGCCGGCCGT) and (GCAAGCTCTAGACTAGCACTCGCC) as 3' primers to generate genes encoding the complete heavy chain and light chain fragments, respectively. The genes encoding heavy chain and light chain were digested with *BamH* I and *Nhe* I (New England Biolabs), and *Hind* III and *Xba* I (New England Biolabs), and inserted into an expression vector designed for expression of IgG in mammalian cells. The vector encoding IgG was transfected to CHO DG44 cells (Invitrogen) as described previously (Trill, Shatzman *et*

al., 1995). The overexpressed scFv–Fc fusion protein was purified by protein A gel affinity chromatography in accordance with the manufacturer's instructions (Repligen Corp., Cambridge, MA).

Affinity ELISA

96-well half-area microtiter plates were coated with 100 ng of cotinine-BSA for 12 h at 4°C and blocked with 150 μL of 3% BSA in PBS by incubating for 30 min at room temperature. The wells were added with 50 μL of scFv-Fc or IgG and incubated for 1 h at room temperature. After washing with 0.05% PBST, plates were incubated with an HRP-conjugated IgG-Fc specific antibody. 100 μL of ABTS substrate solution was added to each well. The absorbance was measured at 450 nm.

SPR analysis

Affinity of anti-cotinine IgG was measured using BIAcore 2000 (BIAcore AB, Uppsala, Sweden) seentially as described (van der Merwe *et al*., 1994). All experiments were performed at 25℃. Cotinine-BSA was coupled to a CM5 sensor chip using the amine coupling kit (BIAcore AB) at the concentration of 200 μg/mL in 10 mM sodium acetate buffer (pH 4.0). Anti-cotinine IgG was serially diluted in PBS to concentrations ranging from 10 nM to 0.3125 nM. After a binding assay, the chip was regenerated by washing with 5 μL of 50 mM NaOH. Runs at different concentrations of anti-cotinine IgG were performed to obtain data for the association and dissocication rates. The K_D was calculated form kinetic association (k_{on}) and dissociation (k_{off}) constants as: $K_D=k_{off}/k_{on}$.

Competitive enzyme immunoassay for measuring cotinine

Conjugation of cotinine with horseradish peroxidase (HRP)

A mixture containing 17.6 mg (0.10 mmol) of trans-4'-cotininecarboxylic acid (Sigma-Aldrich), 13.9 mg (0.12 mmol) of N-hydroxysuccinimide (Sigma-Aldrich), and 24.3 mg (0.12 mmol) of dicyclohexylcarbodiimide (Sigma-Aldrich) in 1 mL of dimethylformamide (Sigma-Aldrich) was stirred at room temperature for 2 h. After centrifugation at 10,000g for 30 min, 400-μL aliquots of the clear supernatant containing the active ester were diluted with 500 μL of dimethylformamide and slowly added to 2 mL of 50 mmol/L carbonate buffer, pH 9.6, containing 10 mg/mL HRP. This mixture was allowed to react at room temperature for 3.5 h with stirring. The conjugate was dialyzed against PBS for 12 h.

Competitive enzyme immunoassay

The wells of 96-well half-area microtiter plates were coated with anti-cotinine scFv–Fc fusion protein by adding 200 ng of the protein dissolved in 20 μL of PBS to each well and incubating overnight at 4°C. The wells were incubated with 150 μL of 3% BSA in PBS for 1 h and washed with PBS. A mixture of 25 μL of cotinine-HRP conjugate and 25 μL of experimental sample was added to each well, and the plates were incubated for 1 h at room temperature in the dark. The plates were washed five times with dH_2O. To quantify the cotinine-HRP conjugate bound to the plates, 50 μL of 3,3',5,5'-tetramethylbenzidine (TMB) substrate solution (Thermo Fisher Scientific, San Jose, CA) was added to each well. The plates were incubated for 30 min at room temperature in the

dark, and the reaction was then quenched by adding 50 μL of 2M H_2SO_4 to each well. The absorbance was measured at 450 nm.

LC/MS assay

The LC/MS assay was performed at the Department of Life Sciences of the Korea Institute of Science and Technology, as described previously (Kim and Huestis, 2006). The limit of detection (LOD) and LLOQ for LC/MS were 0.5 ng/mL and 1 ng/mL, respectively.

Collection of human serum

Human serum samples were collected from 36 volunteers with informed consent from all participants. All methods were approved by the ethics committee of the National Cancer Center in accordance with the Declaration of Helsinki.

Monitoring serum cotinine concentration in rats injected with nicotine

Male Sprague–Dawley rats each weighing 250–300 g were divided into four groups of five animals (A, B, C, and D) and housed in cages with free access to food and water in a temperature- and humiditycontrolled room. Before injection of nicotine or PBS, 600 μL of blood was collected from the tail vein of each rat. The rats in each group were then injected intraperitoneally with 1 mL of PBS containing nicotine (Sigma-Aldrich) as follows: Group A, 20.0 μg/kg; Group B, 2.0 μg/kg; Group C, 0.2 μg/kg; and Group D, 0 μg/kg. At 1, 2, 3, 6, 12, 24, and 48 h after injection, blood was collected from the rats via

the tail vein. The serum was immediately separated and used in competitive ELISA. The animal research was approved by the ethics committee of Seoul National University.

Statistical analysis

To evaluate group differences in the serum cotinine level at 2 h after nicotine injection in the animal study, I used one-way analysis of variance (ANOVA), followed by Fisher's LSD test using SPSS 18 (SPSS Inc., Chicago, IL). The optimal cut-off value was determined with a receiver operating characteristic (ROC) analysis using MedCalc (MedCalc Software, Mariakerke, Belgium). A '$p<0.05$' was considered statistically significant.

In vivo carrier for cotinine conjugated molecule

Peptide synthesis and conjugation with cotinine

Peptides (WKYMVm-NH_2, wkymvm-NH_2) and cotinine-peptide conjugates (cotinine-WKYMVm-NH_2, cotinine-wkymvm-NH_2) used in this study were synthesized by Peptron Inc. (Daejon, South Korea).

Cell culture

Vector- or FPR2-transfected RBL-2H3 cells were maintained in RPMI 1640 (Invitrogen) supplemented with 10% fetal bovine serum (FBS; Invitrogen), 100 U/mL penicillin, and 100 g/mL streptomycin. FPR2-transfected RBL-2H3 cells were also

treated with 250 μg/mL G418.

Reactivity of the cotinine-WKYMVm-NH2/antibody complex to FPR2-transfected RBL-2H3 cell in flow cytometric analysis

FPR2- or vector-transfected RBL-2H3 cells (1×10^5 cells per sample) were washed twice with PBS and once with flow cytometric assay buffer (1% FBS, 0.02% sodium azide in PBS). FPR2-transfected RBL-2H3 cells were incubated with 0, 1, 10, or 100 nM cotinine-WKYMVm-NH_2 and 100 nM anti-cotinine antibody for 30 min at 4°C in 50 μL flow cytometric assay buffer. In parallel control experiments, the cells were incubated with 0, 1, 10, or 100 nM cotinine-WKYMVm-NH_2 and 100 nM control IgG (Palivizumab; Synagis®; Abbot Laboratories, Kent, UK), or 100 nM cotinine-wkymvm-NH_2 and 100 nM anti-cotinine antibody. In another control experiment, vector-transfected RBL-2H3 cells were incubated with 0, 1, 10, or 100 nM cotinine-WKYMVm-NH_2 and 100 nM anti-cotinine antibody. Cells were then washed with flow cytometric assay buffer twice and incubated with FITC-labeled anti-human antibody (Thermo Fisher Scientific, Waltham, MA) diluted 1:100 in 50 μL flow cytometric assay buffer for 20 min at 4°C. After washing twice with flow cytometric assay buffer, the cells were resuspended in 100 μL PBS, fixed with100 μL 2% paraformaldehyde, and analyzed with a FACSCanto™ II flow cytometer (BD Bioscience, Heidelberg, Germany). Data were analyzed with FlowJo data analysis software (Treestar, Ashland, OR, USA).

Isolation of human neutrophils

Peripheral blood was collected from healthy donors, and human neutrophils were isolated by dextran sedimentation, hypotonic lysis of erythrocytes, and a lymphocyte separation medium gradient as described previously (Bae et al., 2001). Isolated neutrophils were maintained in RPMI 1640 medium supplemented 5% FBS at 37°C until used for experiments.

Calcium measurement

Intracellular calcium concentration ($[Ca^{2+}]_i$) was determined by Grynkiewicz's method using Fura-2/AM as described previously (Grynkiewicz et al., 1985). Briefly, freshly isolated human neutrophils were incubated with 3 μM Fura-2/AM at 37°C for 50 min in 4 mL fresh serum-free RPMI 1640 under continuous stirring. After washing three times with serum-free RPMI 1640, 2×10^6 cells were aliquoted for each assay in 1 mL Ca^{2+}-free Locke's solution (154 mM NaCl, 5.6 mM KCl, 1.2 mM $MgCl_2$, 5 mM HEPES [pH 7.3], 10 mM glucose, and 0.2 mM EGTA). The cells were stimulated with 1, 2.5, 5, 10, or 100 nM WKYMVm-NH_2 or cotinine-WKYMVm-NH_2, either alone or with anti-cotinine antibody (molar ratio of 2:1). As negative controls, 100 nM wkymvm-NH_2 or cotinine-wkymvm-NH_2 either alone or with 50 nM anti-cotinine antibody were used. Fluorescence changes were measured at 500 nm at excitation wavelengths of 340 nm and 380 nm using a RF-5301PC spectrofluorophotometer (Shimadzu Instruments Inc., Kyoto, Japan). An increase in intracellular calcium concentration causes an increase in the fluorescence ratio of 340 nm to 380 nm excitation efficiency, and $[Ca^{2+}]_i$ can be calculated using the fluorescence ratio according to equation 5 of Grynkiewicz et al.

Measurement of superoxide generation

Superoxide generation was measured by using the superoxide-dependent reduction of cytochrome c as described previously (Bae et al., 2001). Human neutrophils (2×10^6 cells in RPMI 1640) were preincubated with 50 μM cytochrome c at 37°C for 1 min and then incubated with 10, 100, or 1,000 nM WKYMVm-NH_2 or cotinine-WKYMVm-NH_2, either alone or with anti-cotinine antibody (molar ratio of 2:1). As negative controls, 10, 100, and 1,000 nM wkymvm-NH_2 or cotinine-wkymvm-NH_2, either alone or with anti-cotinine antibody (molar ratio of 2:1), were used. The absorption changes with cytochrome c reduction at 550 nm were recorded using a spectrophotometer (EL312e; Bio-Tek instruments, Winooski, VT) over 5 min at 1-min intervals. The initial absorbance value (0 min) was subtracted from each subsequent reading, and this value was converted to nanomoles of superoxide by dividing the absorbance by an extinction coefficient of 0.022 μM-1cm-1.

Chemotaxis assay

Chemotaxis assays were performed using multiwell chambers (Neuroprobe, Gaithersburg, MD) as described previously (Bae et al., 2001). Briefly, prepared human neutrophils were suspended in RPMI at a concentration of 1×10^6/mL, and 25 μL of this suspension was placed onto the upper wells of a chamber separated by a 3-μm polyhydrocarbon filter from the low well, which contained 10 or 100 nM WKYMVm-NH_2 or cotinine-WKYMVm-NH_2, either alone or with anti-cotinine antibody (molar ratio of 2:1). As negative controls, 10 and 100 nM of wkymvm-NH_2 or cotinine-wkymvm-NH_2,

either alone or with anti-cotinine antibody (molar ratio of 2:1), were used. After incubation for 90 min at 37°C, non-migrated cells were removed by scraping, and cells that migrated across the filter were fixed with 4% paraformaldehyde overnight. Fixed filters were dehydrated with 90%, 80%, and 70% ethanol and deionized water for 2 min, sequentially. After dehydration, filters were air-dried, and dried filters were stained with hematoxylin (Sigma-Aldrich, St Louis, MO). Stained cells from each well were counted in five randomly chosen high-power fields (400×) (Bae et al., 2001).

Pharmacokinetic properties of cotinine-WKYMVm-NH2 and cotinine-WKYMVm-NH_2/antibody complex

All experiments involving animals adhered to the guidelines and received the approval of the Institutional Review Committee for Animal Care and Use at Sungkyunkwan University School of Medicine. Pharmacokinetic studies were performed using aged (4-6 weeks old) male wild-type albino Institute of Cancer Research Center (ICR) mice (ORIENT BIO Inc. Seongnam, Korea). To determine the pharmacokinetic property of cotinine-WKYMVm-NH_2 and cotinine-WKYMVm-NH_2/antibody complex, mice were given a single slow-push bolus tail vein injection of cotinine-WKYMVm-NH_2 (0.5 mg/kg) with or without anti-cotinine antibody (10 mg/kg) in a final volume of 100 μL (n=9 mice per bleeding time). Peripheral blood samples (~300 μL) were collected from the retro-orbital plexus at 0, 0.5, 1, 2, 3, 4, 5, 6, 8, 10, 12, 16, 20, and 24 h from cotinine-WKYMVm-NH_2-injected mice and 0, 0.5, 1, 2, 3, 4, 5, 6, 8, 10, 12, 16, 20, 24, 48, 72, 96, 120, 144, and 168 h from cotinine-WKYMVm-NH_2/antibody complex-injected mice. The

relative amount of cotinine-WKYMVm-NH_2 was determined by flow cytometric analysis. Serum samples were diluted (1:5) in 25 μL flow cytometric assay buffer and mixed with 25 μL 200 nM anti-cotinine antibody to allow cotinine-WKYMVm-NH_2 in the diluted sera to complex with the antibody. FPR2-transfected RBL-2H3 cells (1×10^5 cells per sample) were incubated with the mixture for 30 min at 4°C, washed twice with flow cytometric assay buffer, and incubated with FITC-labeled anti-human antibody diluted 1:100 in 150 μL flow cytometric assay buffer for 20 min at 4°C. The cells were washed twice with the flow cytometric assay buffer, resuspended in 100 μL PBS, fixed with 100 μL 2% paraformaldehyde, and subjected to flow cytometry using a FACSCanto™ II flow cytometer (BD Bioscience). Data were analyzed with FlowJo data analysis software. Statistical analysis was performed with GraphPad Prism 5 software for Windows (GraphPad Software, San Diego, CA).

Pharmacokinetic properties of anti-cotinine antibody

Mice were given a single slow-push bolus tail vein injection of anti-cotinine antibody (10 mg/kg) dissolved in 100 μL PBS (n = 3 mice per bleeding time). Peripheral blood samples (~300 μL) were collected from retro-orbital plexus at after 0, 1 , 3, 6, and 12 h, and 1, 2, 3, 4, 5, 6, 7, 10, 14, 21, and 28 days. After incubation at room temperature for 30 min, the samples were centrifuged at 800g for 15 min. The sera were collected and stored at -80°C until analysis. Serum concentrations of anti-cotinine antibody were measured using an enzyme immunoassay. Twenty microliters cotinine-BSA (5 μg/mL) were added to each well of a microtiter plate and incubated overnight at 4°C. After washing with PBS

with 0.05% Tween 20, 150 μL of 3% BSA in PBS was added to each well. After incubation for 1 h at room temperature, 50 μL of diluted serum samples (1:10−1:1,000 dilution) or anti-cotinine antibody solution of known concentrations (50−1,000 ng/mL) was added to each well. The plate was incubated for 1 h at room temperature and washed four times with PBS with 0.05% Tween 20. Then 50 μL/well horseradish peroxidase-conjugated goat anti-human antibody (Thermo Fisher Scientific) diluted 1:5,000 in blocking solution was added. The plate was incubated for 30 min at room temperature and washed five times with PBS with 0.05% Tween 20. ABTS [2, 2′-azino-bis-(3-ethylbenzothiazoline-6-sulphonic acid)] substrate solution (100 μL/well; Amresco, Solon, OH) was added, plates were incubated for 30 min at room temperature, and optical density was measured at 405 nm.

Cecal ligation and puncture

For CLP, ICR mice were anesthetized with ether, and a small abdominal midline incision was made to expose the cecum. The cecum was ligated below the ileocecal valve, punctured once through both surfaces with a 22-gauge needle, and then returned to the central abdominal cavity. Sham-operated mice were subjected to the same procedure, but without ligation or puncture of the cecum. The abdominal incision was closed three layers with 6-0 nylon sutures. Each group was given a single slow-push bolus tail vein injection with cotinine-WKYMVm-NH_2/antibody complex [0.4 mg (240 nmol)/kg or 0.04 mg (24 nmol)/kg cotinine-WKYMVm-NH_2 and 18 mg (120 nmol)/kg or 1.8 (12 nmol) mg/kg anti-cotinine antibody], cotinine-WKYMVm-NH_2 [0.4 mg (240 nmol)/kg], WKYMVm-

NH_2 [0.2 mg (240 nmol)/kg], anti-cotinine antibody [18 mg (120 nmol)/kg] dissolved in 100 μL PBS, or PBS, at 2, 14, 26, and 38 h after CLP. Survival was monitored once daily for 10 days.

Statistical analysis

Survival data were analyzed using the log-rank test with Bonferroni test for post hoc comparisons. Pharmacokinetic data were analyzed using a linear regression test. Statistical significance was set a priori at $p<0.05$.

In vitro carrier for cotinine conjugated molecule

Preparation of aptamer-cotinine conjugates

The aptamer-cotinine conjugates used in this study were synthesized by Postech Aptamer Initiative (Pohang, South Korea) using the active ester method as described previously (Park et al.), purified to homogeneity (i.e., <95% purity) by reversed-phase high-pressure liquid chromatography with an Xbridge Prep C18 column (5 μm, 10 × 150 mm, Waters Corp., Milford, MA), and assessed by mass spectrometry. The quality of conjugated aptamers was analyzed with an ion-trap mass spectrometer through electrospray ionization (ESI-IT/MS) by Postech Aptamer Initiative (Pohang, South Korea). AS1411-cotinine and CRO26-cotinine conjugates were dissolved in water; pegaptanib-cotinine conjugates were dissolved in diethyl pyrocarbonate-treated water. Dissolved aptamer-cotinine conjugates were annealed at 95°C for 5 min and slowly

cooled to 25°C over 30 min. All conjugates were aliquoted and stored at -20°C until use.

Cell culture

Raji (human Burkitt's lymphoma), HepG2 (human hepatocellular carcinoma), U87MG (human glioblastoma), and NIH3T3 (mouse embryonic fibroblast) cells were grown in RPMI 1640 (GIBCO) culture media containing 10% fetal bovine serum (FBS; GIBCO), 100 U/mL penicillin, and 100 g/mL streptomycin at 37°C in 5% CO_2.

Flow cytometric analysis

Raji, HepG2, U87MG, and NIH3T3 cells (1×10^5 cells/mL) were resuspended in 100 μL flow cytometric assay buffer [1% FBS and 0.02% sodium azide in phosphate-buffered saline (PBS)] and incubated with the indicated concentrations of AS1411-cotinine and 100 nM anti-cotinine antibody at 4°C for 20 min. As a control, CRO26-cotinine and palivizumab were used in place of AS1411-cotinine and anti-cotinine antibody, respectively. After washing twice with flow cytometric assay buffer, cells were incubated with FITC-labeled anti-human IgG (Thermo Fisher Scientific) at 4°C for 15 min and washed again with flow cytometric assay buffer. The cells were fixed with PBS containing 2% paraformaldehyde; fluorescence intensity was measured using FACSCanto™ II (BD Bioscience, Heidelberg, Germany) and analyzed with FlowJo data analysis software (Treestar, Ashland, OR, USA).

Immunoblot analysis using aptamer

Raji cell lysate (50 μg) was dissolved in 4× SDS loading buffer (50 mM MES, 50 mM Tris-base, 0.1% SDS, 1 mM EDTA, and 50 mM dithiothreitol, pH 7.3) and separated by 4–12% gradient SDS-polyacrylamide gel electrophoresis (SDS-PAGE) followed by transfer onto a nitrocellulose membrane (Whatman, Dassel, Germany) using an XCell SureLock™ Novex Mini-Cell (Invitrogen) at 40 V for 60 min. The membrane was pre-incubated in TBST (10 mM Tris, pH 7.5, 150 mM NaCl, and 0.1% Tween-20) containing 5% non-fat milk (BD Biosciences Diagnostic Systems, Sparks, MD) at room temperature for 30 min and then incubated with 100 nM AS1411-cotinine/50 nM anti-cotinine antibody complexes, 100 nM AS1411-cotinine/50 nM control antibody complexes, 100 nM CRO26-cotinine/50 nM anti-cotinine antibody complexes, or a 1:100 dilution of mouse anti-nucleolin antibody (Santa Cruz Biotechnology) at room temperature for 2 h. After the membrane was washed three times with TBST, it was incubated with either HRP-conjugated mouse or rabbit anti-human IgG (Thermo Fisher Scientific) diluted 1:5,000 in TBST at room temperature for 1 h. The membrane was washed three times with TBST, and protein bands were visualized by the addition of SuperSignal Pico West chemiluminescent substrate (Thermo Fisher Scientific) following the manufacturer's instructions.

Oligonucleotide immunoprecipitation using aptamer

Raji cells were harvested by centrifugation at 168g for 3 min at 4°C and then washed three times with PBS. The pellet was resuspended in 1 mL lysis buffer (20 mM Tris-Cl, pH 7.5, 150 mM NaCl, 1% Triton X-100, 0.25 mM synthetic dextrose complete medium, 1 mM PMSF, 1 μg/mL aprotinin, 1 μg/mL leupeptin, and 1 μg/ml pepstatin A) and

sonicated for three rounds, 10 s each at an output setting of 7 (Sonic Dismembrator model 500, Thermo Fisher Scientific). The sonicated samples were cleared by centrifugation for 10 min at 17,000g, and the amount of protein in the supernatants was measured by Bradford assay (Bio-Rad, Richmond, CA). The cell lysate (1 mg) was incubated with 40 nM AS1411-cotinine/20 nM anti-cotinine antibody complexes, 40 nM CRO26-cotinine/20 nM anti-cotinine antibody complexes, or 40 nM AS1411-cotinine/20 nM control antibody complexes at 4°C overnight on an end-over-end rotator. Protein A-sepharose beads (40 μL, Repligen) were added to the lysate mixture and incubated with rotation for 2 h at 4°C. After this incubation, the immunoprecipitates were washed three times with wash buffer (20 mM Tris-Cl, pH 7.5, 150 mM NaCl, and 1% Triton X-100), resuspended in 4× SDS loading buffer, and denatured at 95°C for 10 min. All samples were analyzed by SDS-PAGE and transferred onto a nitrocellulose membrane. The membrane was blocked with 5% nonfat milk in TBST and then treated with mouse anti-nucleolin IgG (1:100; Santa Cruz Biotechnology). After the membrane was washed three times with TBST, it was incubated with HRP-conjugated rabbit anti-mouse IgG diluted 1:5,000 in TBST at room temperature for 1 h. The membrane was washed three times with TBST, and protein bands were visualized by the addition of the SuperSignal Pico West chemiluminescent substrate (Thermo Fisher Scientific) following the manufacturer's instructions.

Enzyme immunoassays using aptamer

The wells of microtiter plates were coated by the addition of 50 ng human VEGF

dissolved in 20 μL PBS to each well for an overnight incubation at 4°C. The wells were incubated with 150 μL of 3% BSA in PBS for 2 h and then washed with PBS. Subsequently, both the 100 nM pegaptanib-cotinine/50 nM anti-cotinine antibody complex and 100 nM bevacizumab were serially diluted 10-fold in PBS containing 3% BSA and added to each well. The plates were incubated for 1 h at room temperature and then washed five times with 0.05% PBST. Subsequently, a 50-μL aliquot of HRP-conjugated rabbit anti-human IgG (Thermo Fisher Scientific), diluted 1:5,000 in PBS with 3% BSA, was added to each well and incubated for 1 h at room temperature. After washing four times with 0.05% PBST, peroxidase activity was detected by the addition of 50 μL TMB substrate solution to each well. The plates were incubated for 10 min at room temperature, and the absorbance at 650 nm was measured using a Multiskan Ascent instrument (Labsystems, Helsinki, Finland).

Results

Generation of anti-cotinine-antibody

In immunization with antigen, it was important to determine the titer of antibody in serum with regular intervals during the course of injections, since a strong antibody titer will result in a pool of RNA and cDNA, which is enriched for antigen-binding immunoglobulin genes that make up the building blocks of a combinatorial antibody library (Barbas CF, 3rd *et al*., 2001). In order to measure the titer of serum antibody, serum samples withdrawn from rabbit were applied to ELISA. The antibody titer reached an appropriate level after eighth round of injection (Fig. 9). Total RNA was extracted from rabbit bone marrow and spleen and then rabbit immune scFv library was constructed using overlap PCR. Using phage display, scFv clone was selected from library. Then its reactivity against cotinine was examined in simple indirect and competitive phage ELISA. As result of indirect ELISA, selected scFv specifically bound to cotinine conjugated carrier protein (Fig. 10A). In a competitive ELISA the binding of the scFv was inhibited by addition of free cotinine in a dose dependent manner (Fig. 10B). The scFv gene was successfully converted into scFv-Fc and full length IgG with retaining original affinity (Fig. 11, Fig. 12). The affinity of full IgG was determined in a real-time interaction analysis using BIAcore system. The calculated values for k_{on}, k_{off}, and K_D were 2.599×10^{6}, 1.253×10^{-5}, and 4.896×10^{-12} (Fig. 13).

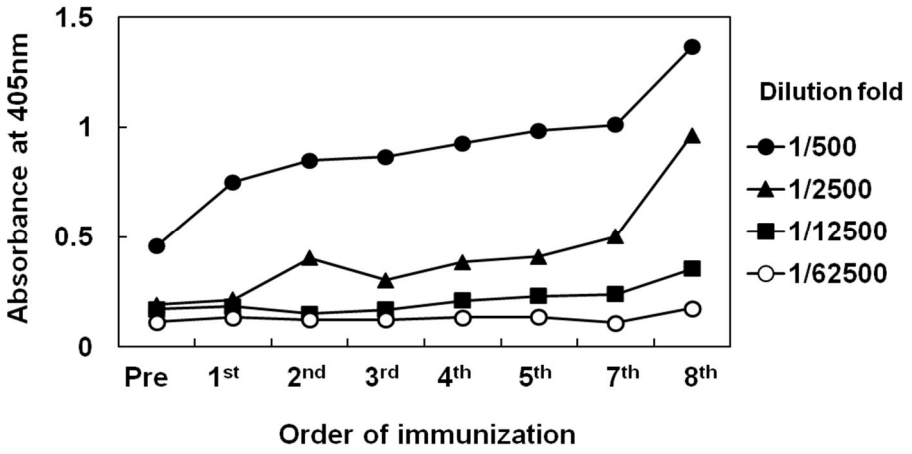

Figure 9. Titration of serum antibodies against cotinine.

5-fold serum dilutions of both of pre- and immunized serums were prepared and allowed to react with cotinine-BSA immobilized on the microtiter plate. HRP-conjugated goat anti-rabbit IgG and ABTS substrate solution were employed to determne the amount of serum antibody bound to the microtiter plate.

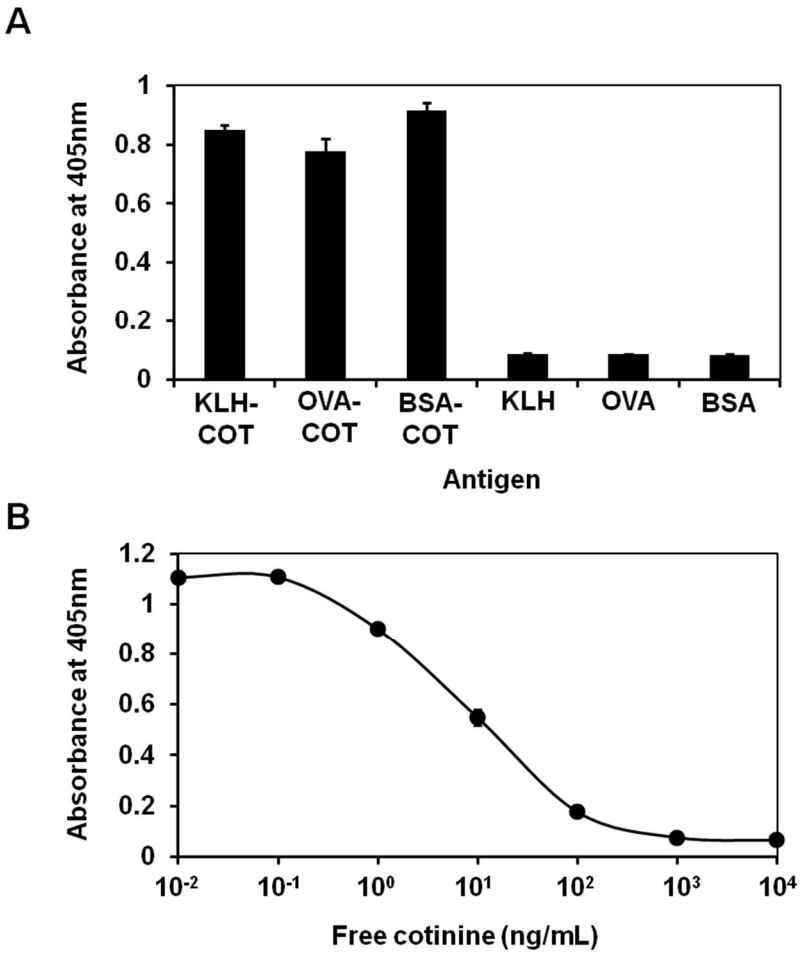

Figure 10. Specific reactivity of scFv phage clone against cotinine.

(A) Selected scFv phage clone was allowed to react with cotinine-carrier protein conjugates or carrier proteins on the microtiter plate. HRP-conjugated anti-M13 antibody and ABTS substrate solution were employed to determine the amount of antibody binding

to the microtiter plate. The results are expressed as the mean ± S.D. of triplicate measurements. (B) Selected scFv phage clone was mixed with free cotinine and allowed to react with cotinine-BSA immobilized on the microtiter plate. HRP-conjugated anti-M13 antibody and ABTS substrate solution were employed to determine the amount of antibody binding to the microtiter plate. The results are expressed as the mean ± S.D. of triplicate measurements.

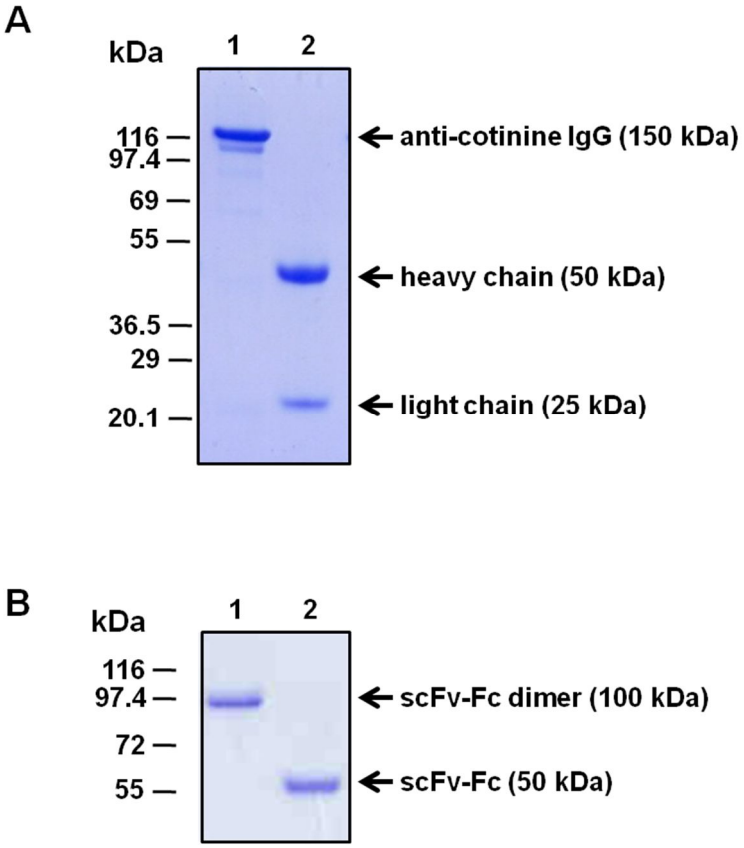

Figure 11. Coomassie staining of purified anti-cotinine IgG and scFv-Fc under non-denaturing and denaturing conditions.

(A) Non-denatured (lane 1) and denatured (lane 2) anti-cotinine IgG were subjected to 4–12% SDS-PAGE and gel was stained with Commassie billiant blue to visualize the bands. (B) Non-denatured (lane 1) and denatured (lane 2) anti-cotinine scFv-Fc were subjected to 4–12% SDS-PAGE and gel was stained with Commassie billiant blue to visualize the bands.

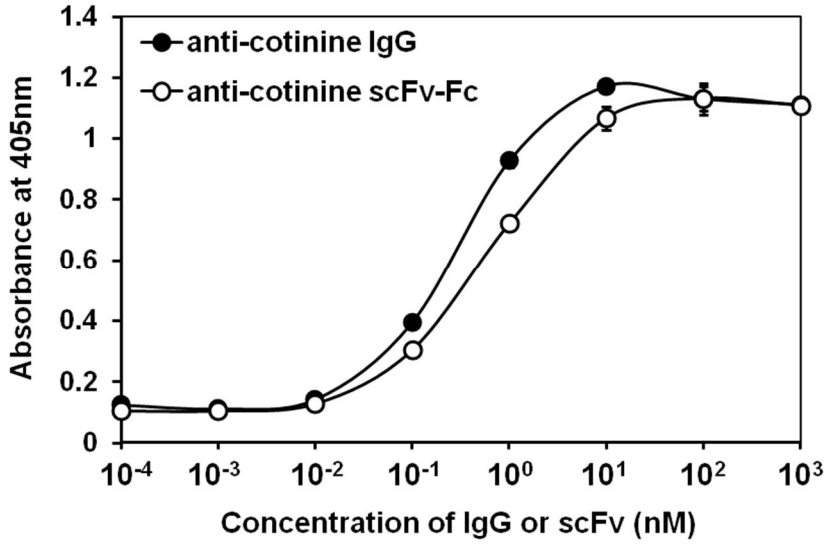

Figure 12. Comparision of binding affinity between IgG and scFv-Fc against cotinine.

Anti-cotinine IgG and scFv-Fc antibody were serially diluted and allowed to react with cotinine-BSA immobilized on the microtiter plate. HRP-conjugated anti-human IgG antibody and ABTS substrate solution were employed to determine the amount of antibody binding to the microtiter plate. The results are expressed as the mean ± S.D. of triplicate measurements.

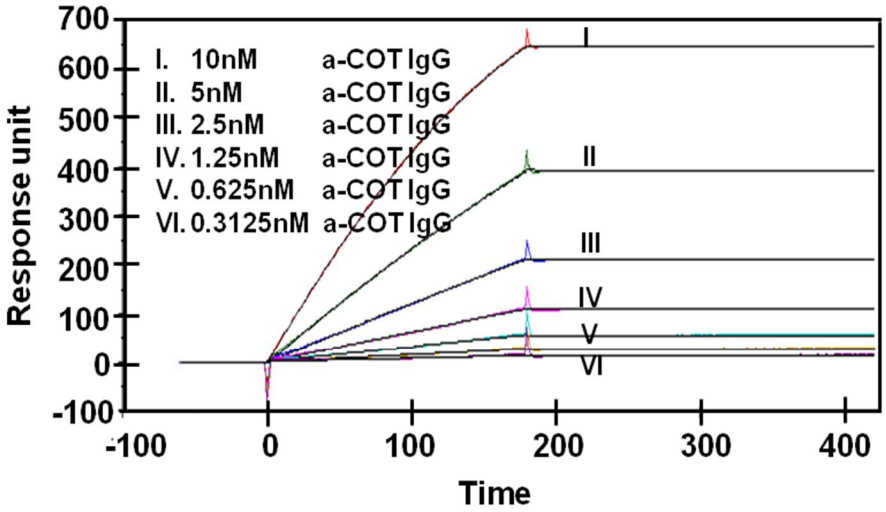

K_D (M)	4.896×10^{-12}
K_{on}	2.599×10^{6}
K_{off}	1.253×10^{-5}

Figure 13. Real time interaction analysis of anti-cotinine IgG with the cotinine.

Cotinine-BSA was immobilized on a CM5 sensor chip by using an amine coupling kit and the anti-cotinine IgG was injected at 10 μL/mL for 60 s over the biosensor chip. From the data obtained, the rate constants and K_D were calculated.

Enzyme immunoassay for measuring cotinine

Characterization of the ELISA

The calibration curve for the competitive ELISA (n=6) (Fig. 14) was generated with 12 different cotinine concentrations, ranging from 0 to 10,000 ng/mL. The CV was between 2.6% and 10.8% over the range of 1 to 1,000 ng/mL. The LOD, defined as the lowest cotinine concentration detectable in the assays, was calculated as ±3 SD for six replicates of the zero calibrator. The LLOQ was the lowest cotinine concentration calculated on the basis of the lowest concentration that gave a CV of ≤20%. In the competitive ELISA, the LOD and LLOQ were 31 pg/mL and 1 ng/mL, respectively (Fig. 15). To determine the intraassay precision, I included 12 calibrators and 3 QC samples in each assay and analyzed 7 replicates. The intra-assay CVs were 13.5%, 3.8%, and 10.2% for the samples with low (1.5 ng/mL), middle (7.5 ng/mL), and high (500.0 ng/mL) concentrations of QC, respectively. In addition, to assess the inter-assay precision over a 28-day period, I included 10 calibrators and 3 QC samples in each assay and analyzed 40 runs in duplicate. The respective inter-assay precisions were 14.0%, 14.4%, and 15.0% (Table 4). Nicotine, anabasine, caffeine, albumin, and cholesterol, diluted in rabbit serum, showed no crossreactivity with the anti-cotinine antibody at concentrations below 25 ng/mL.Trans-3'-hydroxy cotinine exhibited cross-reactivity at concentrations above 89 ng/mL and negligible cross-reactivity below 25 ng/mL. Recoveries after the addition of cotinine to serum without cotinine were 97% for 1 ng/mL, 93% for 10 ng/mL, 95% for 100 ng/mL, and 118% for 1000 ng/mL.

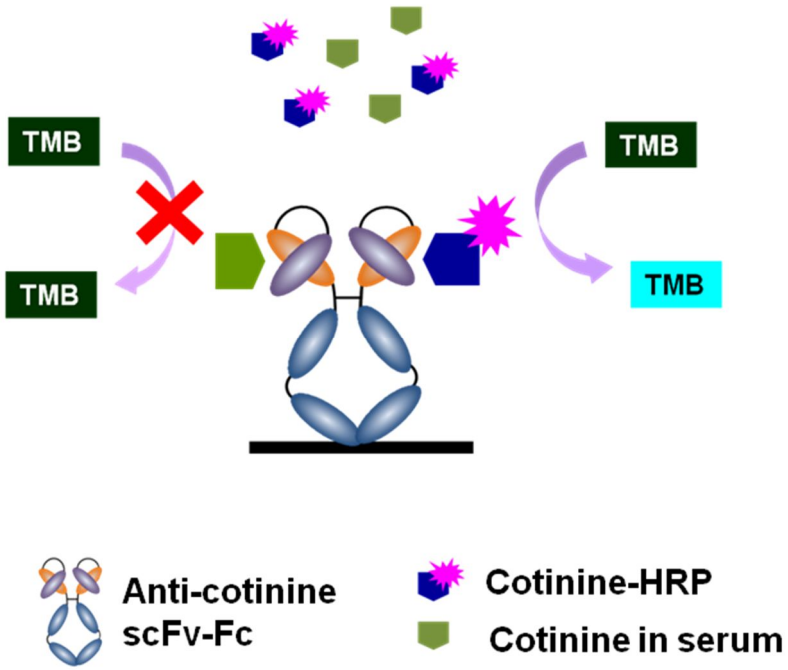

Figure 14 . Concept of competitive enzyme immunoassay.

Purified anti-cotinine IgG was bound to the microtiter plate. Probing was carried out in the presence of samples or dilutions of free antigen (standards) with HRP conjugated cotinine. The HRP conjugated cotinine competes with the free cotinine, reducing the amount of antibody bound. Comparison between samples and standards yields quantitative information.

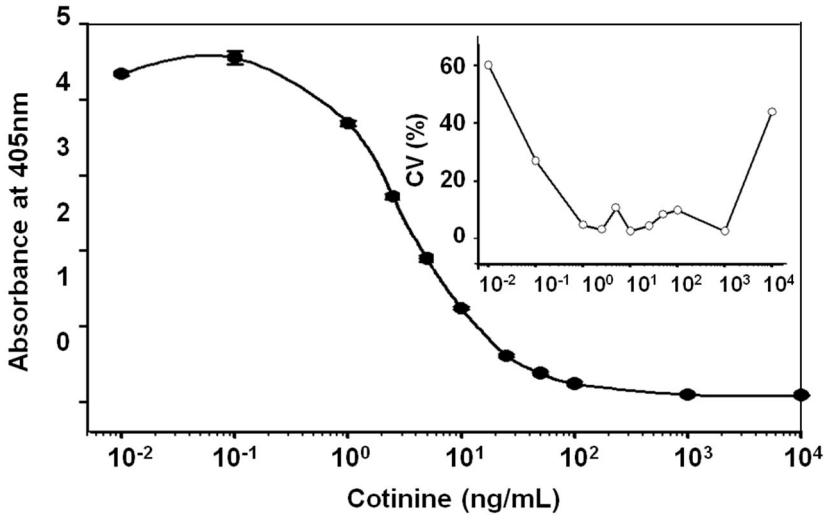

Figur 15. Standard curve and precision profile for cotinine.

12 calibrators and HRP conjugated cotinine were allowed to react with anti-cotinine scFv-Fc immobilized on the microtiter plate. TMB substrate solution was employed to determine the amount of antibody binding to the microtiter plate. The results are expressed as the mean ± S.D. of triplicate measurements.

Table 4. Imprecisions in the cotinine quantitation assays.

QCs (ng/mL)	Intra-assay				Inter-assay			
	n	Mean (ng/mL)	SD (ng/mL)	CV (%)	n	Mean (ng/mL)	SD (ng/mL)	CV (%)
1.5	7	1.56	0.21	13.5	40	1.78	0.25	14.0
7.5	7	8.44	0.32	3.8	40	7.51	1.08	14.4
500.0	7	507.14	51.66	10.2	40	561.04	84.07	15.0

Determination of cotinine in human serum

Thirty-six volunteers were divided into 3 groups, non-, passive, and active smoking, according to their smoking profiles. Human serum samples were collected from the volunteers, and competitive ELISAs were performed twice in triplicate. The samples from non-smoking group contained cotinine at concentrations ranging from 0.93 to 13.71 ng/mL (n=10) and those from passive smoking group had cotinine concentrations ranging from 1.73 ng/mL to 11.50 ng/mL (n=10), and those from active smoking group had cotinine concentrations ranging from 52.94 ng/mL to 933.00 ng/mL (n=16).

For diagnosis of smoking level, I performed ROC analysis of cotinine in non- and passive smoking groups, non- and active smoking groups, and passive and active groups. Sensitivity and specificity were determined for three comparements were represented in table 5. The area under the curve (AUC) for the ROC curve was reported 0.745, 1.000, and 1.000, respectively (Table 6). The cut off value of this ELISA was 5.1 ng/mL. The diagnostic significance of cotinine showed significance.

Table 5. Sensitivity and specificity according to ELISA for detecting smoking level in humas serums.

	Smoking level			Sensitivity (%)			Specificity (%)		
	Non (n=10)	Passive (n=10)	Active (n=16)	Passive vs. Non	Active vs. Non	Active vs. Passive	Passive vs. Non	Active vs. Non	Active vs. Passive
Cotinine									
Positive	2	6	16	60	100	100	90	100	100
Negative	8	4	0						

Table 6. Area under the receiver operating characteristic curves (AUC) for diagnosis of smoking level in human serums.

(p<0.05, Receiver operating characteristic (ROC) analysis)

	Passive vs. Non	Active vs. Non	Active vs. Passive
AUC (95% CI)	0.745 (0.493-0.904)	1.000 (0.881-1.000)	1.000 (0.868-1.000)
p value	<0.05	-	-

Comparison of the competitive ELISA and LC/MS

To compare the performance of the competitive ELISA with that of a previously available assay (LC/MS) for determination of cotinine concentration in serum, I performed split-sample assays with serum samples containing four different concentrations of cotinine. I prepared stock rabbit serum containing 14.00 ng/mL cotinine and serially diluted it with rabbit serum to obtain samples with cotinine concentrations of 7.00, 3.50, and 1.75 ng/mL. Each prepared sample was divided into 10 aliquots; 5 of these were analyzed using competitive ELISA, whereas the remaining five were analyzed using LC/MS. The intra-assay imprecisions of ELISA and LC/MS for each of five replicate runs were represented in Table 7.

Table 7. Comparision of intra-assay imprecision of ELISA and LC/MS for each of five replicate runs.

Samples (ng/mL)	n	ELISA			LC/MS		
		Mean (ng/mL)	SD (ng/mL)	CV (%)	Mean (ng/mL)	SD (ng/mL)	CV (%)
1.75	5	1.78	0.24	13.54	1.83	1.60	87.5
3.50	5	4.02	0.52	12.91	2.60	0.72	27.6
7.00	5	6.91	0.81	11.72	7.40	1.81	24.5
14.00	5	14.93	1.60	10.70	15.36	0.79	5.1

Monitoring serum cotinine concentrations in rats injected with nicotine

To simulate passive smoking, rats were injected intraperitoneally with 20, 2, 0.2, or 0 μg/kg of nicotine; these nicotine doses are equivalent to the amounts of nicotine absorbed by a 60-kg person who has smoked one cigarette, one-tenth of a cigarette, one-hundredth of a cigarette, or no cigarettes, respectively (Russell *et al.*, 1980). Serum samples were obtained periodically and analyzed by competitive ELISA. Two hours after nicotine injection, the rats that received 20.0 μg/kg showed peak cotinine concentrations of 36.7 to 23.5 ng/ml, while the peak concentrations in rats injected with 2.0 μg/kg were between 7.0 and 3.9 ng/ml, which were significantly different from those of controlled rats ($p<0.005$, $p<0.005$, respectively). Only two of the five rats injected with 0.2 μg/kg nicotine showed a noticeable increase in serum cotinine. And the serum cotinine concentration was significantly different between the 20.0 and 2.0 μg/kg groups ($p<0.005$) and between the 2.0 and 0.2 μg/kg groups ($p<0.05$) (Fig. 16).

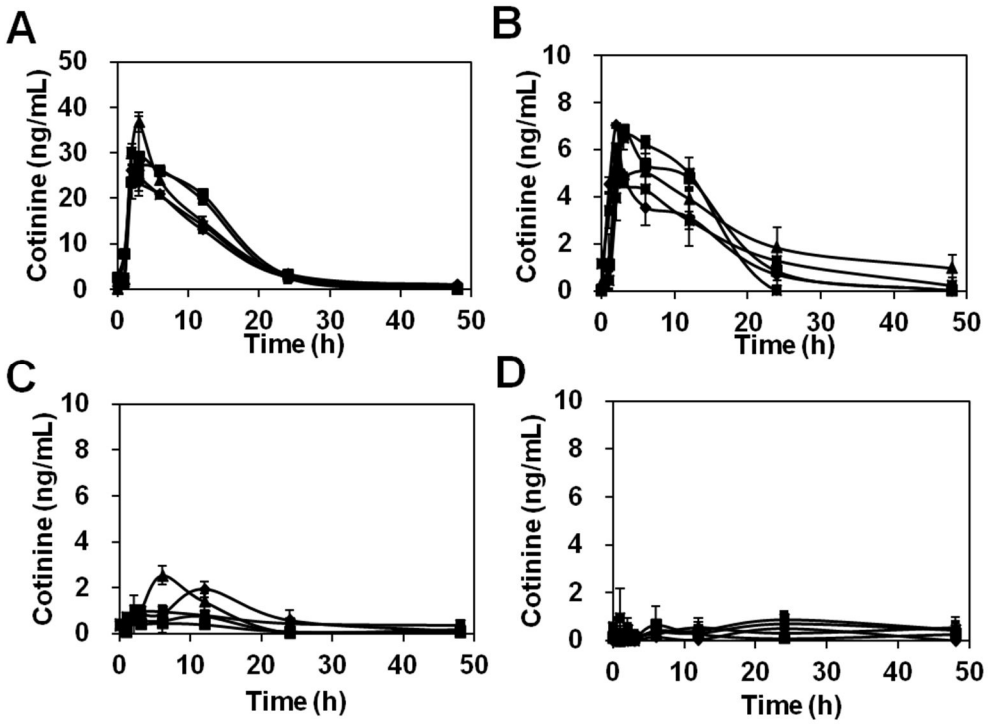

Figure 16. Kinetics of changes in cotinine levels in rats injected with nicotine.

Each group consisted of five SD rats injected intraperitoneally with nicotine. (A) 20.0 μg/kg, (nicotine equivalent to that of one cigarette smoked by a person). (B) 2.0 μg/kg. (C) 0.2 μg/kg; and (D) PBS. The results are expressed as the mean ± S.D. of triplicate measurements. The group differences in the serum cotinine level at 2 h after nicotine injection was $p<0.005$, $p<0.005$, $p<0.005$, and $p<0.05$ in (A) from (D), (B) from (D), (A) from (B), and (B) from (C), respectively ($p<0.05$, one-way analysis of variance (ANOVA), followed by Fisher's LSD test).

In vivo carrier for cotinine conjugated molecule

Retaining functional activity of cotinine conjugated WKYMVm-NH_2 in complex

The peptide Trp-Lys-Tyr-Met-Val-D-Met-$CONH_2$ (WKYMVm-NH_2) (Baek et al., 1996; Kim *et al.*, 2009)) is a synthetic agonist of the formyl peptide receptor (FPR) family and has been proven effective in treating sepsis in an animal model(Kim et al., 2010). However, injection of large amounts of the peptide (4 mg/kg) was required due to its short half-life.

In this study, I conjugated the WKYMVm-NH_2 peptide to cotinine and then tested whether the conjugated peptide within an anti-cotinine rabbit/human chimeric antibody (Park *et al.*) complex would retain its characteristics and exhibit therapeutic efficacy at lower doses. After WKYMVm-NH_2 was chemically synthesized and conjugated to carboxy-cotinine with a linker (Fig. 17), the reactivity of the cotinine-WKYMVm-NH_2/anti-cotinine IgG complex to FPR2 was monitored by flow cytometry using FPR2-transfected RBL-2H3 cells. The cotinine-WKYMVm-NH_2/anti-cotinine IgG complex reacted specifically to FPR2-transfected RBL-2H3 cells, but no reaction was observed when control IgG or cotinine-D-Trp-D-Lys-D-Tyr-D-Met-D-Val-D-Met-$CONH_2$ (wkymvm-NH_2), a negative control peptide, was used (Fig. 18).

I then determined whether the cotinine-WKYMVm-NH_2/anti-cotinine IgG complex retained the functional activity of the peptide in three *in vitro* assays before testing it *in vivo*. Not only cotinine-WKYMVm-NH_2 but also the cotinine-WKYMVm-NH_2/anti-cotinine IgG complex strongly induced Ca^{2+} mobilization in human neutrophils, showing maximal activity around 5 nM (Fig. 19). The observed concentration-dependencies were

very similar to that of WKYMVm-NH_2. Both cotinine-WKYMVm-NH_2 and cotinine-WKYMVm-NH_2/anti-cotinine IgG complex also strongly stimulated superoxide anion production from human neutrophils, showing similar concentration-dependencies as WKYMVm-NH_2 (Fig. 20). The chemotactic activity of WKYMVm-NH_2 was also retained by cotinine-WKYMVm-NH_2 and cotinine-WKYMVm-NH_2/anti-cotinine IgG complex. All three compounds induced chemotactic migration of FPR2-expressing RBL-2H3 cells but did not induce migration of vector-expressing RBL-2H3 cells (Fig. 21). In the three *in vitro* assays above, wkymvm-NH_2, cotinine-wkymvm-NH_2 conjugate, and cotinine-wkymvm-NH_2/anti-cotinine IgG complex, used as negative controls, showed no significant activity. Taken together, these results suggest that neither the conjugation of WKYMVm-NH_2 to cotinine nor the formation of a complex with anti-cotinine antibody hindered the functional activity of WKYMVm-NH_2 as an agonist for FPR2.

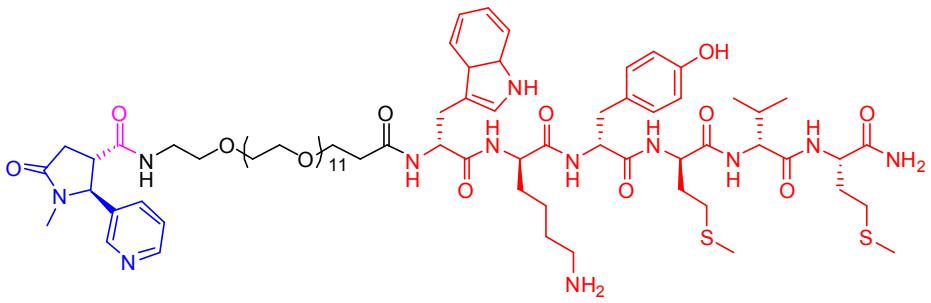

Figure 17. WKYMVm-NH_2 conjugated to cotinine with a linker.

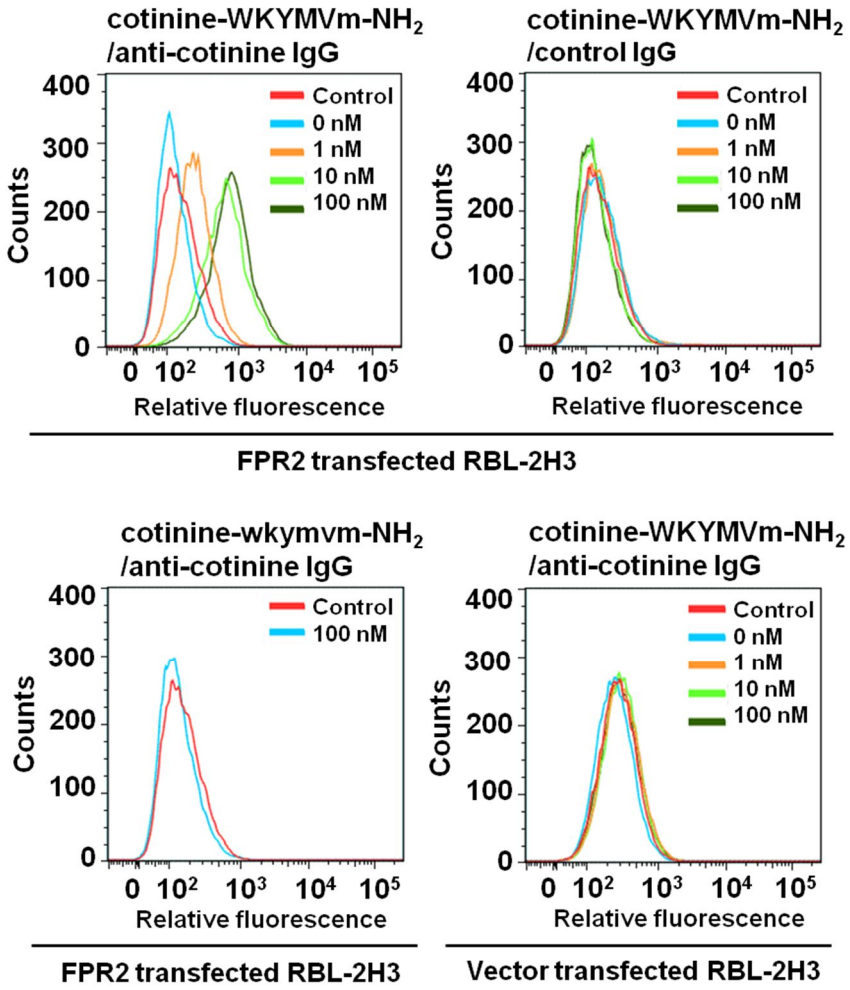

Figure 18. Reactivity of cotinine-WKYMVm-NH_2/anti-cotinine IgG complex to FPR2-transfected RBL-2H3 cell.

FPR2- or vector-transfected RBL-2H3 cells (1×10^5 cells/mL) were incubated with the indicated agents and FITC-labeled anti-human antibody at 4°C for 20 min and subjected to flow cytometric analysis.

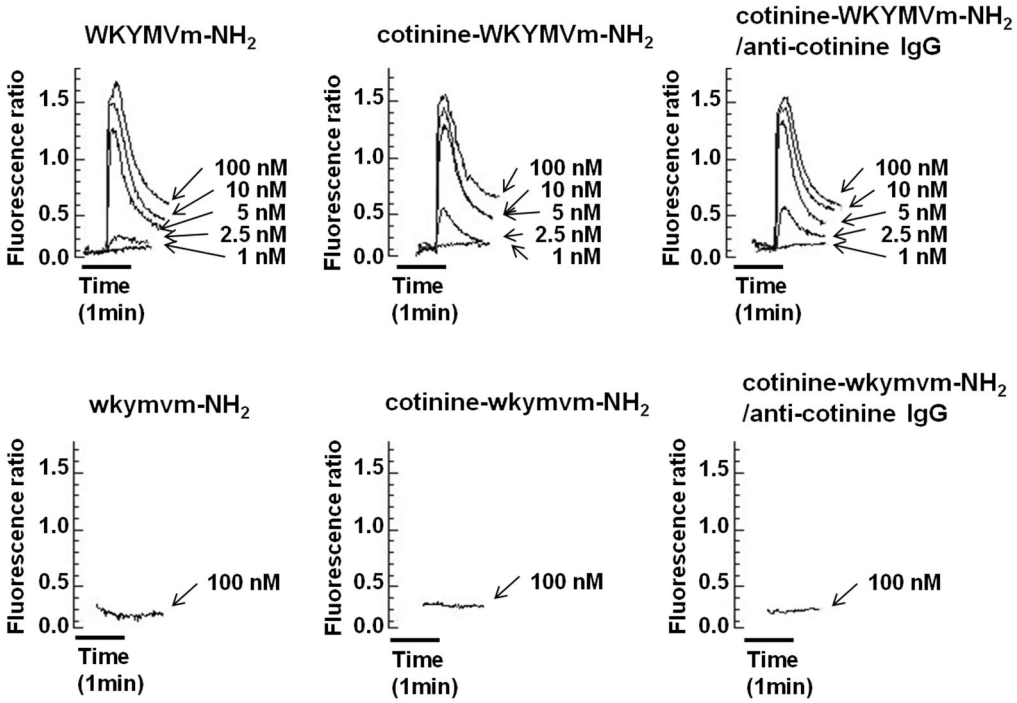

Figure 19. Changes in intracellular calcium concentration ($[Ca^{2+}]_i$) of human neutrophils (2×10^6 cells per assay).

Fura-2-loaded human neutrophils (2×10^6 cells/assay) were stimulated with various concentrations of WKYMVm-NH_2 or other agents. The change in fluorescence ratio (340/380 nm) was monitored. The results are representative of three independent experiments.

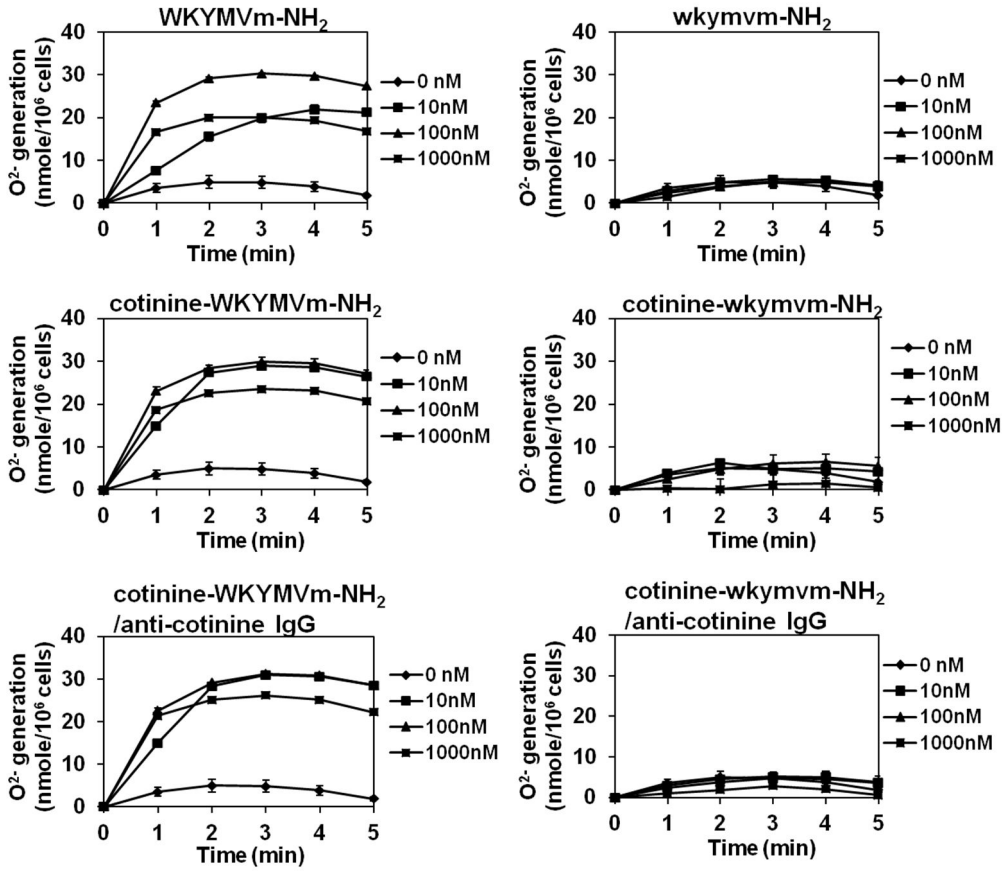

Figure 20. Superoxide generation by treatment of the cotinine-WKYMVm-NH_2/anti-cotinine antibody complex.

Human neutrophils were stimulated with the different agents in the presence of cytochalasin B (5 μM). The amount of superoxide generated was measured using the cytochrome c reduction assay. The results are expressed as the mean ± S.E. of three independent experiments.

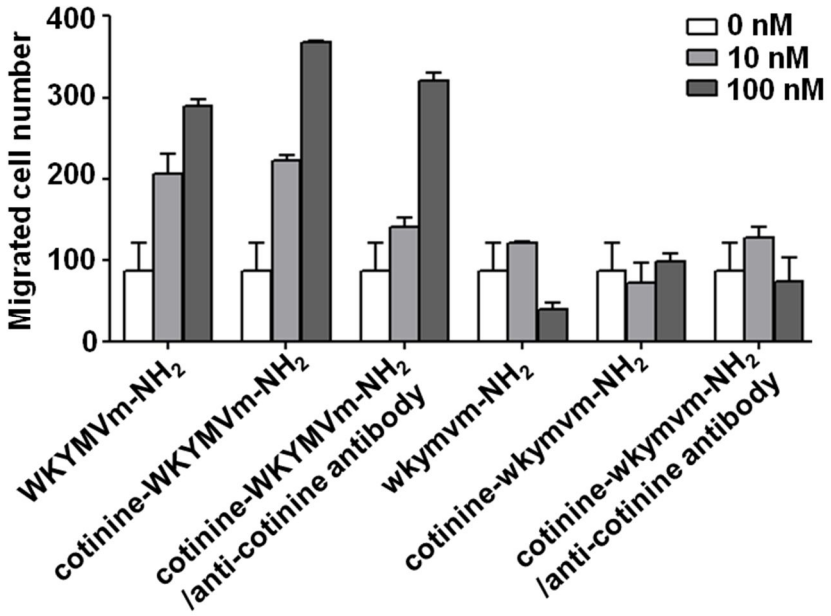

Figure 21. Chemotaxis by treatment of the cotinine-WKYMVm-NH_2/anti-cotinine antibody complex.

Isolated human neutrophils (1×10^6 cells/ml in serum-free RPMI) were added to the upper wells of a 96-well chemotaxis chamber and migration across the polycarbonate membrane was assessed after 1.5 h at 37°C. Migrated cells were counted in a high power field (400×). The results are expressed as the mean ± S.E. of three independent experiments.

Prolonged pharmacokinetics of peptide in complex

I measured the half-life of cotinine-WKYMVm-NH_2/anti-cotinine IgG complex in mice. Cotinine-WKYMVm-NH_2 conjugate (0.5 mg/kg) was injected intravenously with or without anti-cotinine antibody (10 mg/kg), and sera samples were drawn every 4 h for 24 h. Anti-cotinine antibody was then added to sera diluted in flow cytometric assay buffer, which allowed all cotinine-WKYMVm-NH_2 to form a complex with anti-cotinine antibody. The relative amount of WKYMVm-NH_2/anti-cotinine IgG complex was monitored by flow cytometry using FPR2-transfected RBL-2H3 cells. In sera of mice injected with cotinine-WKYMVm-NH_2/anti-cotinine IgG complex, total fluorescence was maintained for 8 h at greater than half its peak value and was above background for 16 h. In contrast, sera of mice injected with cotinine-WKYMVm-NH_2 showed a mean fluorescence decrease to background by 1 h. Using different set of mice, the serum half-life of anti-cotinine antibody was tested. Antibody was injected intravenously at a dose of 10 mg/kg, and sera samples were collected every 96 hours for 28 days (672 h) (Fig 22). The serum half-life of anti-cotinine antibody was determined to be greater than 6 days using an enzyme immunoassay (Fig 23).

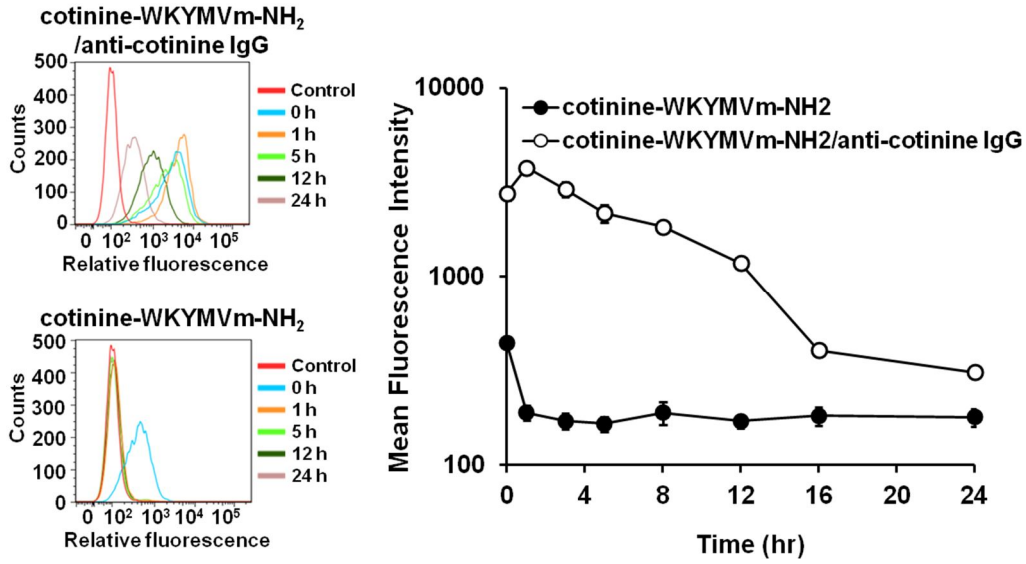

Figure 22. Pharmacokinetic properties of Pharmacokinetic properties of cotinine-WKYMVm-NH_2 and cotinine-WKYMVm-NH_2/anti-cotinine IgG complex.

Cotinine-WKYMVm-NH_2 (0.5 mg/kg) was intravenously injected into mice alone (n=9) or with anti-cotinine antibody (10 mg/kg; n=9). Relative reactivity of sera to FPR2-transfected RBL-2H3 cells was monitored by flow cytometry after addition of excess anti-cotinine antibody. The results are expressed as the mean ± S.E. of nine independent experiments. The linear regression equations of cotinine-WKYMVm-NH_2/anti-cotinine IgG complex and cotinine-WKYMVm-NH_2 are $y=-138.26x+3114.2$, with $r=0.80$ ($P<0.005$) and $y=-4.7564x+252.79$, with $r=0.17$, respectively ($p<0.05$, Linear regression test).

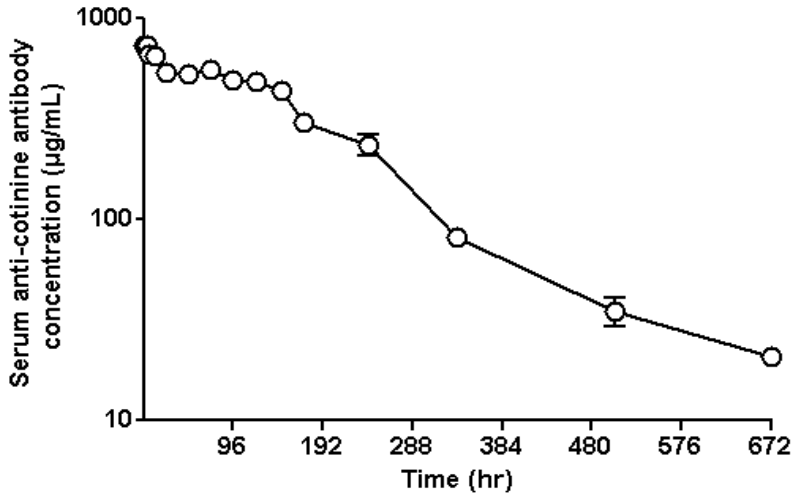

Figure 23. Pharmacokinetic property of anti-cotinine antibody.

After intravenous injection of mice (n=3) with anti-cotinine antibody (10 mg/kg), serum anti-cotinine antibody concentrations were measured by enzyme immunoassay. The results are expressed as the mean ± S.E. of three independent experiments.

Improvement of the therapeutic efficacy of cotinine conjugated peptide

The therapeutic efficacy of cotinine-WKYMVm-NH_2/anti-cotinine IgG complex against sepsis was determined using the cecal ligation-puncture (CLP) animal model(Kim et al.). Institute for Cancer Research mice (N=120) were anesthetized, and a small abdominal midline incision was made to expose the cecum. The cecum was ligated below the ileocecal valve and punctured once through both surfaces with a 22-gauge needle, and the abdomen was closed. Immediately after the procedure, the mice were divided into six groups (n=20). Every 12 h for 2 days, cotinine-WKYMVm-NH_2/anti-cotinine IgG complex [0.4 mg (240 nmol)/kg or 0.04 mg/kg cotinine-WKYMVm-NH_2 and 18 mg (120 nmol)/kg or 1.8 mg/kg anti-cotinine antibody], cotinine-WKYMVm-NH_2 [0.4 mg (240 nmol)/kg], WKYMVm-NH_2 [0.2 mg (240 nmol)/kg], anti-cotinine antibody [18 mg (120 nmol)/kg], or phosphate-buffered saline (PBS) was injected intravenously in a volume of 100 μL. The sham-operated mice were not treated. With 80% of mice surviving over 10 days, the group treated with 0.4 mg/kg cotinine-WKYMVm-NH_2/anti-cotinine IgG complex showed significantly improved survival compared with the group treated with 0.2 mg/kg WKYMVm-NH_2 (45%; $p = 0.0241$) and the group injected with PBS (20%; $p = 0.0001$) (Fig. 24).

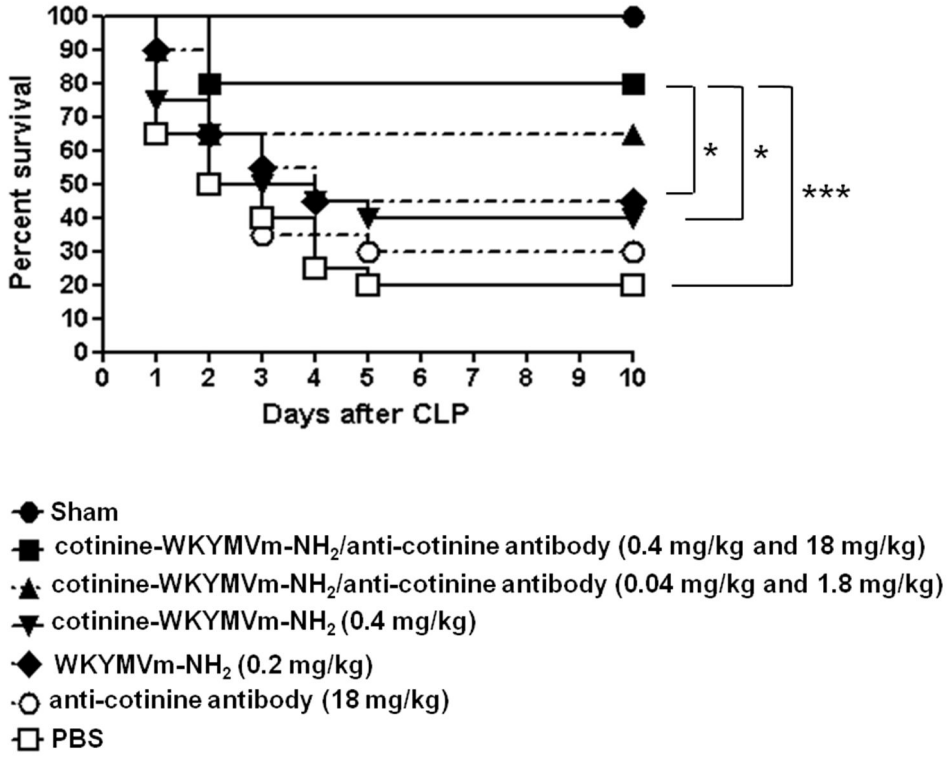

Figure 24. Efficacy of cotinine-WKYMVm-NH_2 and cotinine-WKYMVm-NH_2/anti-cotinine IgG complex induced protection against sepsis.

Various doses of the indicated agents (n=20 mice/group) were injected intravenously 2, 14, 26, and 38 h after CLP, and survival was monitored for 10 days. Asterisks (*) indicate

significant differences from the cotinine-WKYMVm-NH_2/anti-cotinine antibody (0.04 mg/kg and 1.8 mg/kg) or cotinine-WKYMVm-NH_2 (0.2 mg/kg) treated groups ($p<0.05$, Log-rank test with Bonferroni test for post hoc comparisons). Triple asterisks (***) indicate significant differences from the PBS treated group ($p<0.05$, Log-rank test with Bonferroni test for post hoc comparisons).

In vitro carriert for cotinine conjugated molecule

Binding of AS1411-cotinine/anti-cotinine antibody complexes to cell-surface nucleolin

To assess whether AS1411-cotinine/anti-cotinine antibody complexes (Fig. 25, Fig. 26) bind to nucleolin on cell surfaces, Raji cells were incubated with AS1411-cotinine/anti-cotinine antibody complexes and FITC-labeled anti-human IgG antibodies. With the concentration of anti-cotinine antibody fixed at 100 nM, cotinine-conjugated AS1411 at concentrations of 1, 10, and 100 nM bound to the cell surface in a dose-dependent manner. As an IgG molecule, an anti-cotinine antibody contains two paratopes and can form a complex with two molecules of AS1411-cotinine. When either CRO26 or an isotype control for anti-cotinine antibody was used instead of AS1411 or anti-cotinine antibody, respectively, binding of the complex was not observed. CRO26, the negative control of AS1411, is an oligonucleotide in which each dG of AS1411 is replaced by dC, which blocks both the formation of a stable quadruplex structure and nucleolin binding (Soundararajan *et al.*, 2009) (Figure 27A).

I then performed flow cytometric analysis with AS1411-cotinine/anti-cotinine antibody complexes using three additional cell lines that were reported previously to possess different cell surface expression levels of nucleolin (Semenkovich *et al.*, 1990; Hanakahi *et al.*, 1997; Masumi *et al.*, 2006). With 50 nM AS1411-cotinine and 100 nM anti-cotinine antibody, the complex showed stronger binding to HepG2 and U87MG cells and weaker binding to NIH3T3 cells compared to Raji cells (Figure 27B).

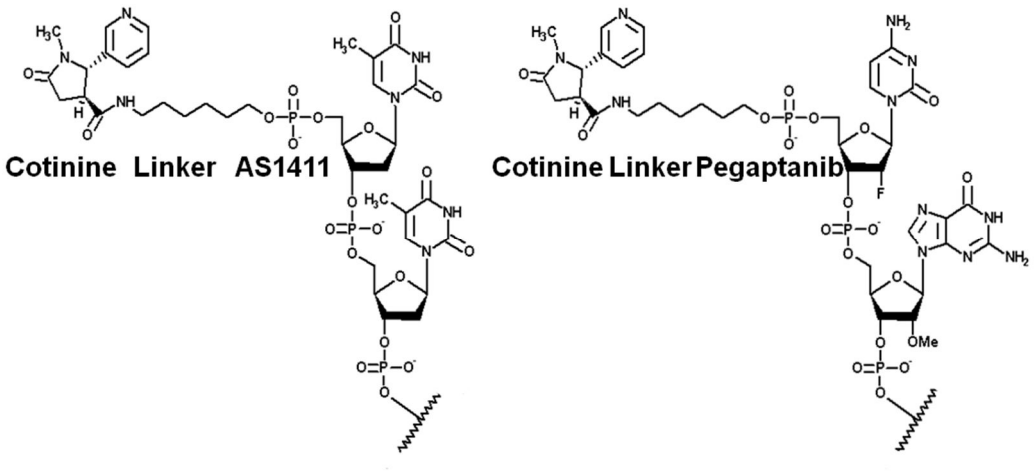

Figure 25. Cotinine-aptamer conjugates.

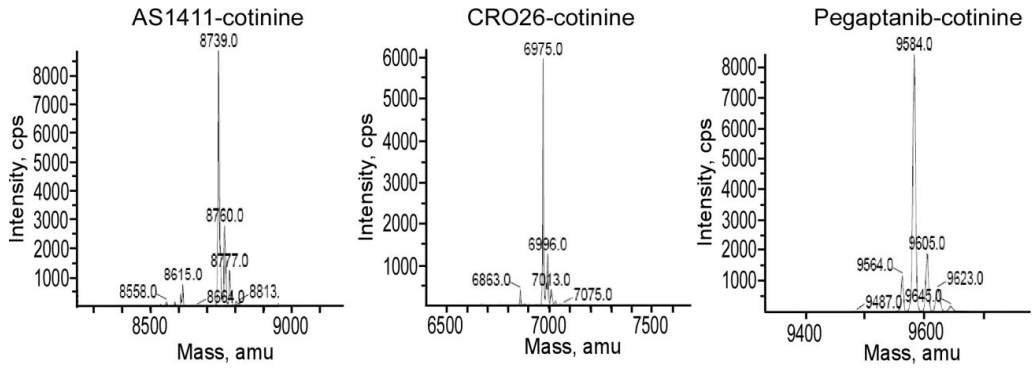

Figure 26. Mass spectroscopy data of aptamer-conjugated cotinine.

The quality of AS1411-cotinine (A), CRO26-cotinine (B), and pegaptanib-cotinine (C) was analyzed using an ion-trap mass spectrometer through electrospray ionization (ESI-IT/MS).

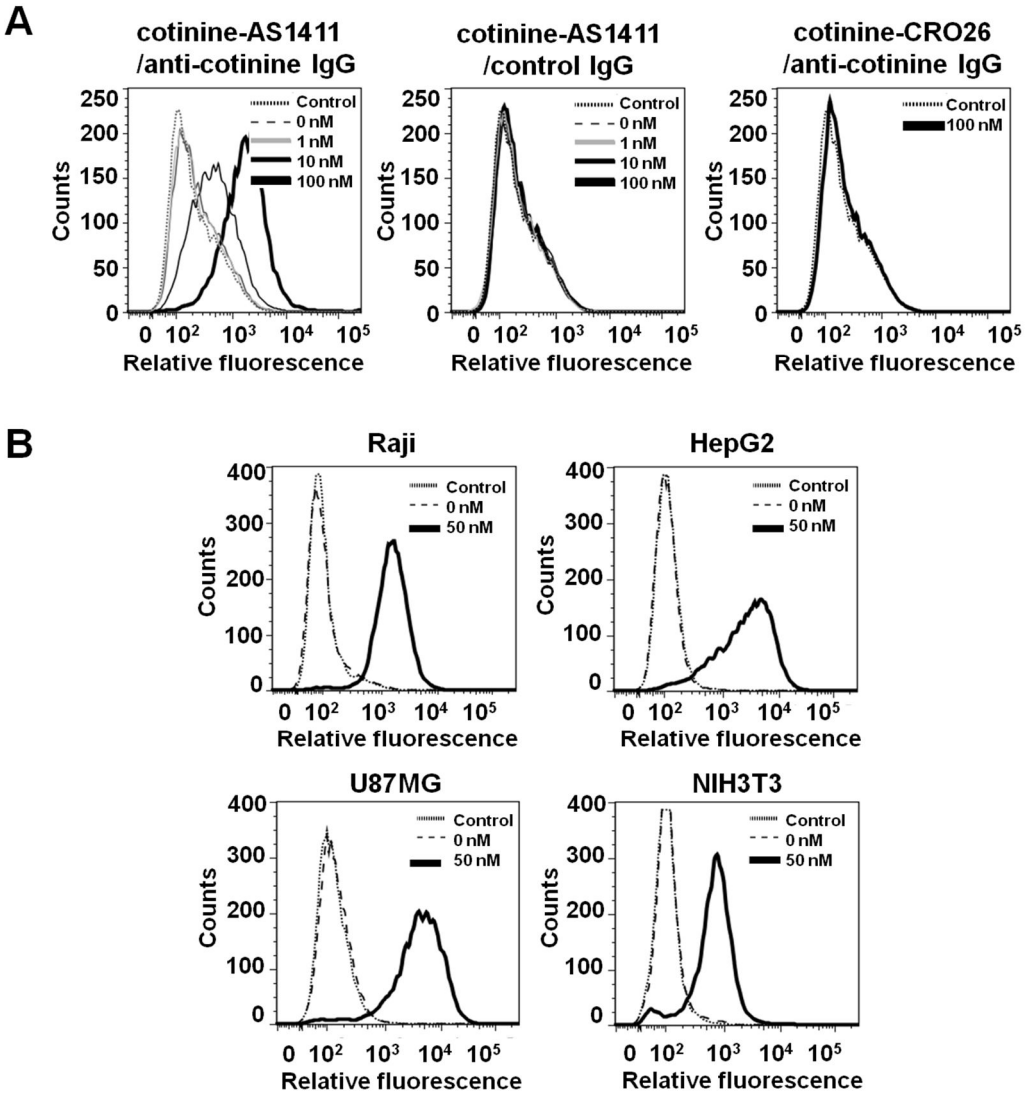

Figure 27. Flow cytometric analysis with AS1411-cotinine/anti-cotinine antibody complexes.

(A) Raji cells were incubated with complexes containing the indicated concentrations of AS1411-cotinine and 100 nM anti-cotinine antibody and subsequently stained with FITC-conjugated anti-human Fc antibody. As a control, CRO26-cotinine and palivizumab were used in place of AS1411-cotinine and anti-cotinine antibody, respectively. Control signal was obtained from cells incubated only with FITC-conjugated anti-human Fc antibody. (B) Raji, HepG2, U87MG, and NIH3T3 cells were incubated with AS1411-cotinine/anti-cotinine antibody complexes and subsequently stained with FITC-conjugated anti-human Fc antibody.

AS1411-cotinine/anti-cotinine antibody complex recognition of denatured nucleolin

To determine whether AS1411-cotinine/anti-cotinine antibody complexes recognize the denatured form of nucleolin, I performed immunoblot analyses. Raji cell lysate (50 μg) was subjected to SDS-PAGE, proteins were transferred to a nitrocellulose membrane, and the membrane was incubated sequentially with AS1411-cotinine/anti-cotinine antibody complexes, HRP-conjugated anti-human IgG antibody, and chemiluminescent substrate solution, with intermittent washing with TBST. AS1411-cotinine/anti-cotinine antibody complexes reacted not only to full-length nucleolin (105 kDa) but also to lower molecular mass forms of nucleolin (<40 kDa) that have been previously reported to be generated by nucleolin autolytic activity (Figure 4A) (Chen *et al.*, 1991; Fang and Yeh, 1993). In contrast, mouse anti-nucleolin antibody reacted only to full-length nucleolin. When either CRO26 or palivizumab was used instead of AS1411 or anti-cotinine antibody, respectively, no bands were visualized (Fig. 28).

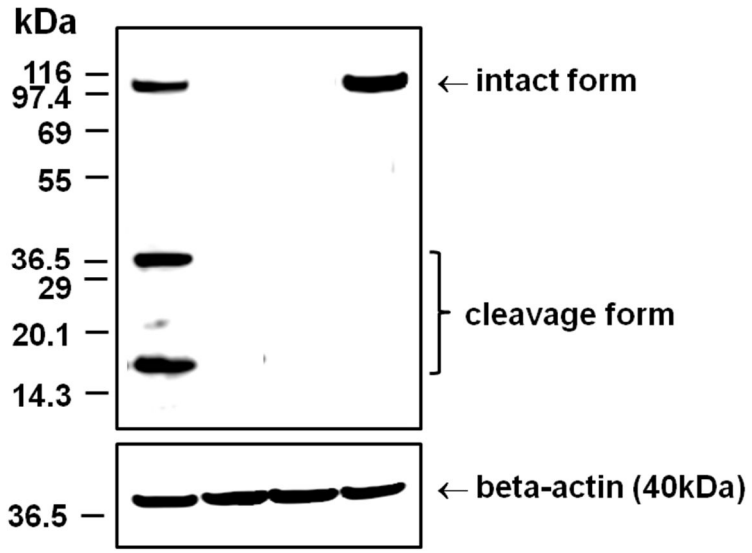

Figure 28. Immunoblot analysis with AS1411-cotinine/anti-cotinine antibody complexes.

Raji cell lysates were subjected to 4–12% SDS-PAGE, and proteins were transferred onto a nitrocellulose membrane. The membrane was probed with AS1411-cotinine/anti-cotinine antibody complexes (lane 1), AS1411-cotinine/control antibody complexes (lane 2), CRO26-cotinine/anti-cotinine antibody complexes (lane 3), and mouse anti-nucleolin antibody (lane 4). HRP-conjugated mouse anti-human IgG, HRP-conjugated rabbit anti-mouse IgG antibody, and SuperSignal Pico West chemiluminescent substrate were used for visualization of the bands.

AS1411-cotinine/anti-cotinine antibody complex immunoprecipitation of nucleolin

Raji cell lysate was incubated with AS1411-cotinine/anti-cotinine antibody complexes overnight. Complexes were then immunoprecipitated using protein A beads and subjected to SDS-PAGE. After the proteins were transferred to a nitrocellulose membrane, immunoblot analysis was performed using anti-nucleolin antibody. A protein band with a molecular weight of 105 kDa was visualized, confirming that AS1411-cotinine/anti-cotinine antibody complexes successfully immunoprecipitated nucleolin from Raji cell lysates. However, when either CRO26 or palivizumab was used instead of AS1411 or anti-cotinine antibody, respectively, no bands were visualized (Fig. 29).

Figure 29. Immunoprecipitation of nucleolin with AS1411-cotinine/anti-cotinine antibody complexes.

Raji cell lysates were incubated with AS1411-cotinine/anti-cotinine antibody complexes (lane 1), AS1411-cotinine/control antibody complexes (lane 2), and CRO26-cotinine/anti-cotinine antibody complexes (lane 3). All lysate mixtures were incubated with immobilized protein A beads, and precipitated proteins were fractionated by SDS-PAGE and probed with mouse anti-nucleolin antibody. In lane 4, the cell lysate was directly loaded onto the gel and probed with mouse anti-nucleolin antibody.

Specific binding of pegaptanib-cotinine/anti-cotinine antibody complexes to VEGF

To verify whether pegaptanib-cotinine/anti-cotinine antibody complexes (Fig.25, Fig. 26) can bind to immobilized $VEGF_{165}$ on a microtiter plate, I performed an enzyme immunoassay using a $VEGF_{165}$-coated microtiter plate, cotinine-conjugated pegaptanib/anti-cotinine antibody complexes, and HRP-conjugated anti-human IgG antibody. Cotinine-conjugated pegaptanib/anti-cotinine antibody complexes bound to $VEGF_{165}$ on the plate in a dose-dependent manner from 10^{-1} to 10^{3} pM (Figure 30). In a parallel experiment, bevacizumab showed dose-dependent binding to $VEGF_{165}$.

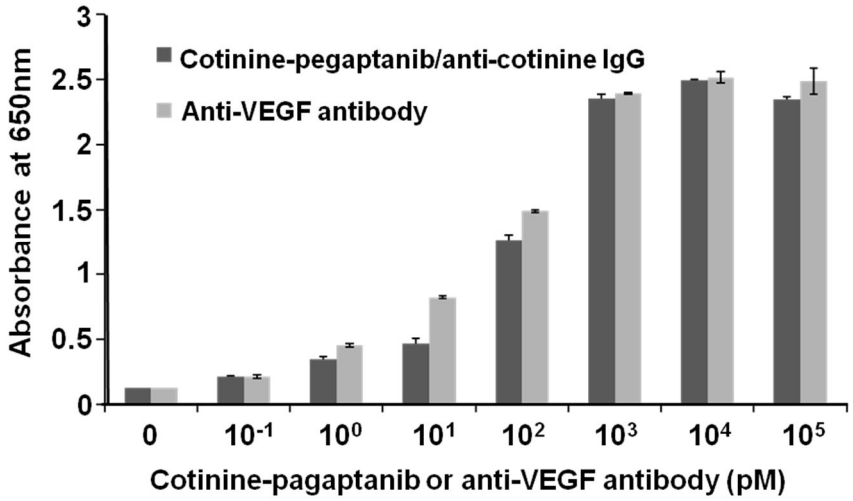

Figure 30. Enzyme immunoassay analysis using pegaptanib-cotinine/anti-cotinine antibody complexes.

Pegaptanib-cotinine/anti-cotinine antibody complexes were allowed to react with $VEGF_{165}$ immobilized on a microtiter plate. The concentration of anti-cotinine antibody was maintained as one-half that of pegaptanib-cotinine as the antibody is bivalent. Bevacizumab was used as a positive control. HRP-conjugated rabbit anti-human IgG antibody and 3,3',5,5'-tetramethylbenzidine substrate solution were employed to determine the amount of complex bound to the microtiter plate. The results are expressed as the mean ± S.D. of triplicate measurements.

Discussion

In this study, I represented the generation of high specific monoclonal antibody against cotinine and the applications of it to enzyme immunoassay for measuring passive smokers and *in vivo* and *in vitro* carrier for cotinine conjugated molecules.

As the start of this study, I focused the hapten, cotinine, for their characteristics as an efficient tobacco biomarker in passive smoking. In a previous study, my co-workers standardized a LC/MS/MS assay for quantifying cotinine in biological samples, including hair, saliva, serum, and urine (Seong *et al.*, 2007; Seong *et al.*, 2008). Using this assay, they showed that paternal smoking inside the home leads to significant maternal and fetal exposure to passive smoking. Based on the need for a more convenient and high-throughput assay for cotinine, I tested three commercially available ELISA kits for their ability to discriminate between passive smokers and nonsmokers. None of these kits were capable of detecting or quantifying typical serum cotinine levels of passive smokers, which ranged between 1 and 15 ng/mL (Seccareccia *et al.*, 2003). This was expected, because the respective LOD and LLOQ values with these kits are 10 and 25 ng/mL in serum; 10 and 500 ng/mL in urine; and 3 and 10 ng/mL in saliva (Hovell *et al.*, 2002). Although radioimmunoassay using rabbit polysera against cotinine can be used to quantify serum cotinine in the range of 0.2–20 ng/mL (Seccareccia et al., 2003), the assay is generally difficult to standardize due to inevitable batch variations in polysera. In the present study, I developed a highly sensitive ELISA that can measure cotinine concentrations in the range of 1 ng/mL to 1 μg/mL, with a CV of ≤15% in standard

samples. The LOD and LLOQ of this assay were 31 pg/mL and 1 ng/mL, respectively, which were comparable to the results of LC/MS assay used in this study. When I applied this ELISA to serum samples from non-, passive, and active smokers, the ELISA represented smoking exposure by 5.1 ng/mL of cut-off value. And I also performed a replicate assay on four split samples. The CVs for the ELISA were between 10.7 and 13.54 and more correct than to those for the LC/MS assay performed in this study. In previous studies using LC/MS/MS to analyze serum samples with cotinine levels lower than 20 ng/mL, the CVs were also within a reasonable range (7.8–13.8) (Bernert *et al.*, 1997; Byrd *et al.*, 2005). In the present study, the relatively higher CVs obtained in the LC/MS assay were likely due to technical difficulties associated with the assay (Beyer *et al.*, 2007). To further confirm that the ELISA can be used to detect and quantify cotinine levels that reflect a low degree of passive exposure to tobacco smoke, I injected rats with various amounts of nicotine and monitored the serum cotinine concentrations. I detected serum cotinine in all of the rats that received more than 2.0 μg/kg nicotine, which is equivalent to passive exposure to the smoke from one-tenth of a cigarette in humans (Lerman *et al.*, 2006). The serum cotinine concentration peaked 2 h after injection of nicotine at a dose equivalent to that in the smoke from one cigarette; the levels of cotinine (23.5–36.7 ng/mL) were equivalent to the levels reported previously (Shoaib and Stolerman, 1999).

Then as another application of anti-cotinine antibody, I developed novel platform as a carrier of cotinine conjugated molecules that is applicable to use *in vivo* and *in vitro*. If an anti-cotinine antibody has a reasonably low K_{off} constant toward cotinine, it can form a

very stable complex with various cotinine-conjugated molecules (e.g., protein, peptide, aptamer, chemical substance) and make the cotinine-conjugated molecule persist much longer in than the molecule alone.

The *in vivo* carrier system is a novel drug delivery system for therapeutic peptide to overcome the deficiencies of PEGylation method including polydipersivity, low loading of PEG, and process development. This system is made of two parts: cotinine and chemically conjugated peptide with linker that gives antigenic reactivity and anti-cotinine antibody that give usual characteristics of antibody. The cotinine conjugated with peptide can mediate the formation of cotinine-peptide/anti-cotinine antibody complex. This complex can retain the original characteristics of both the molecule and the antibody. These characteristics include the specific reactivity and functions of the peptide and long *in vivo* half-life of antibody, activation of complement-mediated cell cytotoxicity (CDC), and antibody-dependent cell cytotoxicity (ADCC). In addition, this complex functions as a new type of antibody where antigenic reactivity of the antibody is determined by the cotinine-conjugated peptide. The feature of this novel drug delivery system is the simplicity of production in that it uses one monoclonal antibody that bind against cotinine with highly specificity. The cotinine that is easily available and common material and peptide that can be quickly and easily synthesized in a high-throughput manner were site-direct conjugated using universal method and assembled with anti-cotinine antibody by simply incubation. Although I showed peptide as the main molecular targeting agent for this system, other molecules including oligonucleotides, chemicals, saccharides, and proteins, can be used as well. Therefore, once a clinical-grade anti-cotinine antibody

production system is established, prior production of an anti-cotinine antibody and a high-throughput production of cotinine conjugated molecular targeting agents would be a much quicker and easier method than PEGylation or the de novo development of new therapeutic antibodies. In present study, I tested novel delivery system using WKYMVm-NH_2 immune-stimulating synthetic peptide which is FPR family agonist and effectively prevent development of sepsis. In previous studies, it is reported that survival of CLP-sepsis mouse was greatly improved when 4 mg/kg WKYMVm-NH_2 was administrated every 12h for 2 days after CLP (Kim *et al.*, 2010). However, 4 mg/kg may be too high amount for clinical practice. In this study, I demonstrated that cotinine-WKYMVm-NH_2/anti-cotinine antibody complex significantly improved therapeutic effect when one tenth amount of typical dose was injected caused by prolonged half-life of the peptide while retained their functional activity. Another feature of this drug delivery system is suggested that this platform is quicker way to generate therapeutic antibodies once a clinical-grade anti-cotinine antibody production system is established. A molecular targeting agent can be developed and produced as a form of a peptide, an aptamer, a small molecule that can be quickly and easily synthesized in a high-throughput manner in a clinical grade. After conjugation with cotinine, the cotinine-conjugated molecule can be allowed to form a cotinine-conjugated molecule/anti-cotinine antibody complex. Prior production of an anti-cotinine antibody and a high-throughput production of cotinine conjugated molecular targeting agents would be a much quicker and easier method than the de novo development of new therapeutic antibodies, since this method usually requires a long period of time to establish production cell lines.

The *in vitro* carrier system is another affinity unit for biological assays using aptamer. For application of aptamers in multiple assays and experiments, biotin labeling has been the most commonly adopted option to avoid the need to develop optimal aptamer cross-linking conditions for multiple enzymes, dyes, or sensors individually (Ramos *et al.*, 2007; Li *et al.*, 2009). Because biotin is stable and small (molecular weight of 244.31 Da), it rarely interferes with the function of labeled molecules. The avidin-biotin detection system allows an aptamer to be easily captured, recovered, immobilized, or detected with a limited number of secondary detection reagents generated by modifying avidin, streptavidin, or neutravidin. A major limitation of this system is that biotin, as vitamin B7, is present in small amounts in all living cells and participates in many biological processes including cell growth and the citric acid cycle (Bender, 1999). Biotin is especially abundant in tissues such as brain, liver, and blood, and endogenous biotin can cause considerable background noise in assays based on biotin binding (Ramos-Vara, 2005). Digoxigenin also has been used to label aptamers for use in biological assays (Dapic *et al.*, 2002). It is a steroid with a low molecular weight of 390.51 kDa that is found exclusively in the flowers and leaves of plants such as *Digitalis purpuea*, *Digitalis orientalis*, and *Digitalis lanata*. Additionally, digoxigenin is a hapten with high immunogenicity (Holtke *et al.*, 1995). It also has served as a standard immunohistochemical marker for in situ hybridization (Hauptmann and Gerster, 1994). For labeling of atpamers, digoxigenin can be conjugated to a nucleotide triphosphate, and the labeled nucleotide triphosphate is then used in aptamer synthesis. The resulting digoxigenin-labeled aptamer can form a complex with anti-digoxigenin antibody for

applications in assays and experiments. Based on several of its characteristics, I selected and tested cotinine as a candidate hapten for labeling aptamers. Because cotinine has a low molecular weight of 176.22 Da, I hypothesized that it would not alter the function of an aptamer upon conjugation. Both cotinine-conjugated AS1411 and cotinine-conjugated pegaptanib retained their reactivity to their original targets in this study. As both cotinine and its binding molecules are not present physiologically in animal and human tissues, minimal background signal was expected. The AS1411-cotinine/anti-cotinine antibody complex recognized denatured nucleolin with minimal background. Taken together, the results demonstrate that cotinine-conjugated aptamer/anti-cotinine antibody complexes can be used in such applications as flow cytometric, immunoblot, immunopreciptation, and enzyme immunoassay analyses, providing a viable alternative for employing cotinine-labeled aptamers in multiple assays and experiments, alone or in combination with biotin- and/or digoxigenin-labeled aptamers in such investigations.

From this study, I concluded that the enzyme immunoassay kit using anti-cotinine antibody is high specificific and sensitive to detect passive smoking level in serum and cotinine conjugated molecule/anti-cotinine antibody complex platform is simple and powerful drug delivery system or biological assay tool as dependent on conjugated molecule.

References

Arap W, Kolonin MG, Trepel M, Lahdenranta J, Cardo-Vila M *et al.*. Steps toward mapping the human vasculature by phage display. Nat Med 8, 121-127 (2002).

Armitage AK, Dollery CT, George CF, Houseman TH, Lewis PJ *et al.*. Absorption and metabolism of nicotine from cigarettes. Br Med J 4, 313-316 (1975)

Backmann N, Zahnd C, Huber F, Bietsch A, Pluckthun A, *et al.*. A label-free immunosensor array using single-chain antibody fragments. Proc Natl Acad Sci U S A 102, 14587-14592 (2005).

Bae YS, Ju SA, Kim JY, Seo JK, Baek SH *et al.*. Trp-Lys-Tyr-Met-Val-D-Met stimulates superoxide generation and killing of Staphylococcus aureus via phospholipase D activation in human monocytes. J Leukoc Biol 65, 241-248 (1999).

Bae YS, Kim Y, Kim JH, Lee TG, Suh PG *et al.*. Independent functioning of cytosolic phospholipase A2 and phospholipase D1 in Trp-Lys-Tyr-Met-Val-D-Met-induced superoxide generation in human monocytes. J Immunol 164, 4089-4096 (2000).

Bae YS, Kim Y, Kim JH, Suh PG and Ryu SH. Trp-Lys-Tyr-Met-Val-D-Met is a chemoattractant for human phagocytic cells. J Leukoc Biol 66, 915-922 (1999).

Bae YS, Kim Y, Park JC, Suh PG and Ryu SH. The synthetic chemoattractant peptide, Trp-Lys-Tyr-Met-Val-D-Met, enhances monocyte survival via PKC-dependent Akt activation. J Leukoc Biol 71, 329-338 (2002).

Bae, YS, Bae H, Kim Y, Lee TG, Suh PG *et al*.. Identification of novel chemoattractant peptides for human leukocytes. Blood 97, 2854-2862 (2001).

Baek SH, Seo JK, Chae CB, Suh PG and Ryu SH. Identification of the peptides that stimulate the phosphoinositide hydrolysis in lymphocyte cell lines from peptide libraries. J Biol Chem 271, 8170-8175 (2009).

Baldrich E, Acero JL, Reekmans G, Laureyn W and O'Sullivan CK. Displacement enzyme linked aptamer assay. Anal Chem 77, 4774-4784 (2005).

Barbas CF, 3rd, Burton DR, Scott JK, Silverman GJ. Phage Display-A Laboratory Manual. New York: Cold Spring Harbor Press; 2001.

Barbas CF, 3rd, Kang AS, Lerner RA and Benkovic SJ. Assembly of combinatorial antibody libraries on phage surfaces: the gene III site. Proc Natl Acad Sci U S A 88, 7978-7982 (1991).

Bass S, Greene R and Wells JA. Hormone phage: an enrichment method for variant

proteins with altered binding properties. Proteins 8, 309-314 (1990).

Bates PJ, Laber DA, Miller DM, Thomas SD, Trent JO. Discovery and development of the G-rich oligonucleotide AS1411 as a novel treatment for cancer. Experimental and Molecular Pathology 86, 151–164 (2009).

Bates PJ, Kahlon JB, Thomas SD, Trent JO and Miller DM. Antiproliferative activity of G-rich oligonucleotides correlates with protein binding. J Biol Chem 274 26369-26377 (1999).

Bender DA. Optimum nutrition: thiamin, biotin and pantothenate. Proc Nutr Soc 58, 427-433 (1999).

Benowitz NL, Hukkanen J and Jacob P, 3rd. Nicotine chemistry, metabolism, kinetics and biomarkers. Handb Exp Pharmacol 29-60 (2009).

Benowitz NL and Jacob P, 3rd. Daily intake of nicotine during cigarette smoking. Clin Pharmacol Ther 35, 499-504 (1984).

Benowitz NL, Jacob P, 3rd, Fong I and Gupta S. Nicotine metabolic profile in man: comparison of cigarette smoking and transdermal nicotine. J Pharmacol Exp Ther 268, 296-303 (1994).

Bernert JT, Jr., Turner WE, Pirkle JL, Sosnoff CS, Akins JR *et al.*. Development and validation of sensitive method for determination of serum cotinine in smokers and nonsmokers by liquid chromatography/atmospheric pressure ionization tandem mass spectrometry. Clin Chem 43, 2281-2291 (1997).

Beyer J, Peters FT, Kraemer T and Maurer HH. Detection and validated quantification of toxic alkaloids in human blood plasma--comparison of LC-APCI-MS with LC-ESI-MS/MS. J Mass Spectrom 42, 621-633 (2007).

Blank M, Weinschenk T, Priemer M and Schluesener H. Systematic evolution of a DNA aptamer binding to rat brain tumor microvessels. selective targeting of endothelial regulatory protein pigpen. J Biol Chem 276, 16464-16468 (2001).

Borisov SM and Wolfbeis OS. Optical biosensors. Chem Rev 108, 423-461 (2008).

Byrd GD, Davis RA and Ogden MW. A rapid LC-MS-MS method for the determination of nicotine and cotinine in serum and saliva samples from smokers: validation and comparison with a radioimmunoassay method. J Chromatogr Sci 43, 133-140 (2005).

Chen CM, Chiang SY and Yeh NH. Increased stability of nucleolin in proliferating cells by inhibition of its self-cleaving activity. J Biol Chem 266, 7754-7758 (2001).

Chen Z, Tabakman SM, Goodwin AP, Kattah MG, Daranciang D *et al.*. Protein microarrays with carbon nanotubes as multicolor Raman labels. Nat Biotechnol 26, 1285-1292 (2008).

Chomczynski P, Sacchi N. Single-step method of RNA isolation by acid guanidinium thiocyanate-phenol-chloroform extraction. Anal Biochem. 162, 156-159 (1987).

Christophe T, Karlsson A, Dugave C, Rabiet MJ, Boulay F *et al.*. The synthetic peptide Trp-Lys-Tyr-Met-Val-Met-NH2 specifically activates neutrophils through FPRL1/lipoxin A4 receptors and is an agonist for the orphan monocyte-expressed chemoattractant receptor FPRL2. J Biol Chem 276, 21585-21593 (2001).

Cohen S, Yoshioka T, Lucarelli M, Hwang LH and Langer R. Controlled delivery systems for proteins based on poly(lactic/glycolic acid) microspheres. Pharm Res 8, 713-20 (1991).

Cook DG and Strachan DP. Health effects of passive smoking-10: Summary of effects of parental smoking on the respiratory health of children and implications for research. Thorax 54, 357-366 (1999).

D'Angelo E, Rossi P and Garthwaite J. Dual-component NMDA receptor currents at a single central synapse. Nature 346, 467-470 (1990).

Dahlgren C, Christophe T, Boulay F, Madianos PN, Rabiet MJ *et al.*. The synthetic chemoattractant Trp-Lys-Tyr-Met-Val-DMet activates neutrophils preferentially through the lipoxin A(4) receptor. Blood 95, 1810-1818 (2000).

Dapic V, Abdomerovic V, Marrington R, Peberdy J, Rodger A *et al.*. Biophysical and biological properties of quadruplex oligodeoxyribonucleotides. Nucleic Acids Res 31, 2097-2107 (2003).

Dapic V, Bates PJ, Trent JO, Rodger A, Thomas SD *et al.*. Antiproliferative activity of G-quartet-forming oligonucleotides with backbone and sugar modifications. Biochemistry 41, 3676-3685 (2002).

Ellington AD and Szostak JW. In vitro selection of RNA molecules that bind specific ligands. Nature 346, 818-822 (1990).

Fang SH and Yeh NH. The self-cleaving activity of nucleolin determines its molecular dynamics in relation to cell proliferation. Exp Cell Res 1993;208:48-53

Ferreira CS, Papamichael K, Guilbault G, Schwarzacher T, Gariepy J *et al.*. DNA aptamers against the MUC1 tumour marker: design of aptamer-antibody sandwich ELISA for the early diagnosis of epithelial tumours. Anal Bioanal Chem 390, 1039-1050 (2008).

Feyerabend C and Russell MA. A rapid gas-liquid chromatographic method for the determination of cotinine and nicotine in biological fluids. J Pharm Pharmacol 42, 450-452 (1990).

Gao L, Zhuang J, Nie L, Zhang J, Zhang Y *et al.*. Intrinsic peroxidase-like activity of ferromagnetic nanoparticles. Nat Nanotechnol 2, 577-583 (2007).

Gonzalez YM, De Nardin A, Grossi SG, Machtei EE, Genco RJ *et al.*. Serum cotinine levels, smoking, and periodontal attachment loss. J Dent Res 75, 796-802 (1996).

Guo KT, SchAfer R, Paul A, Gerber A, Ziemer G *et al.*. A new technique for the isolation and surface immobilization of mesenchymal stem cells from whole bone marrow using high-specific DNA aptamers. Stem Cells 24, 2220-2231 (2006).

Grynkiewicz, G, Poenie M, Tsien RY. A new generation of Ca^{2+} indicators with greatly improved fluorescence properties. J Biol Chem 260, 3440-3450 (1985).

Hammond SK. Exposure of U.S. workers to environmental tobacco smoke. Environ Health Perspect 107, 329-340 (1999).

Hanakahi LA, Dempsey LA, Li MJ and Maizels N. Nucleolin is one component of the B cell-specific transcription factor and switch region binding protein, LR1. Proc Natl

Acad Sci U S A 94, 3605-3610 (1997).

Hatsukami DK, Grillo M, Pentel PR, Oncken C and Bliss R. Safety of cotinine in humans: physiologic, subjective, and cognitive effects. Pharmacol Biochem Behav 57, 643-650 (1997).

Hauptmann G and Gerster T. Two-color whole-mount in situ hybridization to vertebrate and Drosophila embryos. Trends Genet 10, 266 (1994).

Hawlisch H, Muller M, Frank R, Bautsch W, Klos A *et al.*. Site-specific anti-C3a receptor single-chain antibodies selected by differential panning on cellulose sheets. Anal Biochem 293, 142-145 (2001).

He Y, Lam TH, Jiang B, Wang J, Sai X *et al.*. Passive smoking and risk of peripheral arterial disease and ischemic stroke in Chinese women who never smoked. Circulation 118, 1535-1540 (2008).

Hegaard HK, Kjaergaard H, Moller LF, Wachmann H and Ottesen B. The effect of environmental tobacco smoke during pregnancy on birth weight. Acta Obstet Gynecol Scand 85, 675-681 (2006).

Heimke G, Stock D, Busing CM and von Mallinckrodt D. Biomechanical considerations

on some postoperative problems of directly anchored total hip replacements. J Biomed Mater Res 23, 679-684 (1989).

Holtke HJ, Ankenbauer W, Muhlegger K, Rein R, Sagner G *et al.*. The digoxigenin (DIG) system for non-radioactive labelling and detection of nucleic acids--an overview. Cell Mol Biol (Noisy-le-grand) 41, 883-905 (1995).

Homann M and Goringer HU. Combinatorial selection of high affinity RNA ligands to live African trypanosomes. Nucleic Acids Res 27, 2006-2014 (1999).

Hovell MF, Meltzer SB, Wahlgren DR, Matt GE, Hofstetter CR *et al.*. Asthma management and environmental tobacco smoke exposure reduction in Latino children: a controlled trial. Pediatrics 110, 946-956 (2002).

Hust M, Maiss E, Jacobsen HJ and Reinard T. The production of a genus-specific recombinant antibody (scFv) using a recombinant potyvirus protease. J Virol Methods 106, 225-233 (2002).

Ireson CR and Kelland LR. Discovery and development of anticancer aptamers. Mol Cancer Ther 5, 2957-2962 (2006).

Iribarren C, Darbinian J, Klatsky AL and Friedman GD. Cohort study of exposure to

environmental tobacco smoke and risk of first ischemic stroke and transient ischemic attack. Neuroepidemiology 23, 38-44 (2004).

Iwase A, Aiba M and Kira S. Respiratory nicotine absorption in non-smoking females during passive smoking. Int Arch Occup Environ Health 63, 139-143 (1991).

Jaakkola MS and Jaakkola JJ. Assessment of exposure to environmental tobacco smoke. Eur Respir J 10, 2384-2397 (1997).

Jellinek D, Lynott CK, Rifkin DB and Janjic N. High-affinity RNA ligands to basic fibroblast growth factor inhibit receptor binding. Proc Natl Acad Sci U S A 90, 11227-11231 (1993).

Ji AJ, Lawson GM, Anderson R, Dale LC, Croghan IT *et al.*. A new gas chromatography-mass spectrometry method for simultaneous determination of total and free trans-3'-hydroxycotinine and cotinine in the urine of subjects receiving transdermal nicotine. Clin Chem 45, 85-91 (1999).

Kim I and Huestis MA. A validated method for the determination of nicotine, cotinine, trans-3'-hydroxycotinine, and norcotinine in human plasma using solid-phase extraction and liquid chromatography-atmospheric pressure chemical ionization-mass spectrometry. J Mass Spectrom 41, 815-821 (2006).

Kim SD, Kim JM, Jo SH, Lee HY, Lee SY *et al.*. Functional expression of formyl peptide receptor family in human NK cells. J Immunol 183, 5511-5517 (2009).

Kim SD, Kim YK, Lee HY, Kim YS, Jeon SG *et al.*. The agonists of formyl peptide receptors prevent development of severe sepsis after microbial infection. J Immunol 185, 4302-4310 (2010).

Konthur Z, Hust M and Dubel S. Perspectives for systematic in vitro antibody generation. Gene 364, 19-29 (2005).

Kozlowski LT, Mehta NY, Sweeney CT, Schwartz SS, Vogler GP *et al.*. Filter ventilation and nicotine content of tobacco in cigarettes from Canada, the United Kingdom, and the United States. Tob Control 7, 369-375 (1998).

Krebs B, Rauchenberger R, Reiffert S, Rothe C, Tesar M *et al.*. High-throughput generation and engineering of recombinant human antibodies. J Immunol Methods 254 67-84 (2001).

Larsson ML, Frisk M, Hallstrom J, Kiviloog J and Lundback B. Environmental tobacco smoke exposure during childhood is associated with increased prevalence of asthma in adults. Chest 120, 711-717 (2001).

Le Y, Gong W, Li B, Dunlop NM, Shen W *et al.*. Utilization of two seven-transmembrane, G protein-coupled receptors, formyl peptide receptor-like 1 and formyl peptide receptor, by the synthetic hexapeptide WKYMVm for human phagocyte activation. J Immunol 163, 6777-6784 (1999).

Lee HY, Kang HK, Jo EJ, Kim JI, Lee YN *et al.*. Trp-Lys-Tyr-Met-Val-Met stimulates phagocytosis via phospho-lipase D-dependent signaling in mouse dendritic cells. Exp Mol Med 36, 135-144 (2004).

Lerman C, Tyndale R, Patterson F, Wileyto EP, Shields PG *et al.*. Nicotine metabolite ratio predicts efficacy of transdermal nicotine for smoking cessation. Clin Pharmacol Ther 79, 600-608 (2006).

Li N, Ebright JN, Stovall GM, Chen X, Nguyen HH *et al.*. Technical and biological issues relevant to cell typing with aptamers. J Proteome Res 8, 2438-2448 (2009).

Liu G, Lin YY, Wang J, Wu H, Wai CM *et al.*. Disposable electrochemical immunosensor diagnosis device based on nanoparticle probe and immunochromatographic strip. Anal Chem 79, 7644-7653 (2007).

Machacek DA and Jiang NS. Quantification of cotinine in plasma and saliva by liquid chromatography. Clin Chem 32, 979-982 (1986).

Marks JD, Tristem M, Karpas A and Winter G. Oligonucleotide primers for polymerase chain reaction amplification of human immunoglobulin variable genes and design of family-specific oligonucleotide probes. Eur J Immunol 21, 985-991 (1991).

Masumi A, Fukazawa H, Shimazu T, Yoshida M, Ozato K *et al.*. Nucleolin is involved in interferon regulatory factor-2-dependent transcriptional activation. Oncogene 25, 5113-5124 (2006).

Mateo C, Lombardero J, Moreno E, Morales A, Bombino G *et al.*. Removal of amphipathic epitopes from genetically engineered antibodies: production of modified immunoglobulins with reduced immunogenicity. Hybridoma 19, 463-471 (2000).

McCafferty J, Griffiths AD, Winter G and Chiswell DJ. Phage antibodies: filamentous phage displaying antibody variable domains. Nature 348, 552-524 (1990).

Miyakawa S, Oguro A, Ohtsu T, Imataka H, Sonenberg N *et al.*. RNA aptamers to mammalian initiation factor 4G inhibit cap-dependent translation by blocking the formation of initiation factor complexes. RNA 12, 1825-1834 (2006).

Murphy MB, Fuller ST, Richardson PM and Doyle SA. An improved method for the in vitro evolution of aptamers and applications in protein detection and purification. Nucleic Acids Res 31, e110 (2003).

Nesmeianova MA, Karamyshev AL, Tsfasman IM and Fedotikova ET. [Transformation of various strains of Escherichia coli by multicopy plasmids with the phoA gene leads to secretion of a periplasmatic alkaline phosphatase into the media and accumulation of its precursor]. Mol Biol (Mosk) 25, 770-778 (1991).

Ng EW and Adamis AP. Anti-VEGF aptamer (pegaptanib) therapy for ocular vascular diseases. Ann N Y Acad Sci 1082, 151-171 (2006).

Noppe W, Plieva F, Galaev IY, Pottel H, Deckmyn H *et al.*. Chromato-panning: an efficient new mode of identifying suitable ligands from phage display libraries. BMC Biotechnol 9, 21 (2009).

Oguro A, Ohtsu T, Svitkin YV, Sonenberg N and Nakamura Y. RNA aptamers to initiation factor 4A helicase hinder cap-dependent translation by blocking ATP hydrolysis. RNA 9, 394-407 (2003).

Ohuchi SP, Ohtsu T and Nakamura Y. Selection of RNA aptamers against recombinant transforming growth factor-beta type III receptor displayed on cell surface. Biochimie 88, 897-904 (2006).

Otake Y, Sengupta TK, Bandyopadhyay S, Spicer EK and Fernandes DJ. Retinoid-induced apoptosis in HL-60 cells is associated with nucleolin down-regulation and

destabilization of Bcl-2 mRNA. Mol Pharmacol 67, 319-326 (2005).

Park S, Lee DH, Park JG, Lee YT and Chung J. A sensitive enzyme immunoassay for measuring cotinine in passive smokers. Clin Chim Acta. 411, 1238-1242 (2010).

Pasut G and Veronese FM. State of the art in PEGylation: The great versatility achieved after forty years of research. J Control Release E pub 2011; DOI 10.1016/j.jconrel.2011.10.037.

Perera FP, Mooney LA, Stampfer M, Phillips DH, Bell DA, *et al.*. Associations between carcinogen-DNA damage, glutathione S-transferase genotypes, and risk of lung cancer in the prospective Physicians' Health Cohort Study. Carcinogenesis 23, 1641-1646 (2002).

Perry DC, Davila-Garcia MI, Stockmeier CA and Kellar KJ. Increased nicotinic receptors in brains from smokers: membrane binding and autoradiography studies. J Pharmacol Exp Ther 289, 1545-1552 (1999).

Proske D, Gilch S, Wopfner F, Schatzl HM, Winnacker EL *et al.*. Prion-protein-specific aptamer reduces PrPSc formation. Chembiochem 3, 717-725 (2002).

Ramos-Vara JA. Technical aspects of immunohistochemistry. Vet Pathol 42, 405-426

(2005).

Ramos E, Moreno M, Martin ME, Soto M and Gonzalez VM. In vitro selection of Leishmania infantum H3-binding ssDNA aptamers. Oligonucleotides 20, 207-213 (2010).

Ramos E, Pineiro D, Soto M, Abanades DR, Martin ME *et al.*. A DNA aptamer population specifically detects Leishmania infantum H2A antigen. Lab Invest 87, 409-416 (2007).

Riah O, Dousset JC, Courriere P, Stigliani JL, Baziard-Mouysset G *et al.*. Evidence that nicotine acetylcholine receptors are not the main targets of cotinine toxicity. Toxicol Lett 109, 21-29 (1999).

Richter AW and Akerblom E. Antibodies against polyethylene glycol produced in animals by immunization with monomethoxy polyethylene glycol modified proteins. Int Arch Allergy Appl Immunol 70, 124-131 (1983).

Roberts MJ, Bentley MD and Harris JM. Chemistry for peptide and protein PEGylation. Adv Drug Deliv Rev 54, 459-476 (2002).

Ruckman J, Green LS, Beeson J, Waugh S, Gillette WL *et al.*. 2'-Fluoropyrimidine RNA-

based aptamers to the 165-amino acid form of vascular endothelial growth factor (VEGF165). Inhibition of receptor binding and VEGF-induced vascular permeability through interactions requiring the exon 7-encoded domain. J Biol Chem 273, 20556-20567 (1998).

Russell MA, Jarvis M, Iyer R and Feyerabend C. Relation of nicotine yield of cigarettes to blood nicotine concentrations in smokers. Br Med J 280, 972-976 (1980).

Sakai N, Masuda H, Akitomi J, Yagi H, Yoshida Y *et al.*. RNA aptamers specifically interact with the Fc region of mouse immunoglobulin G. Nucleic Acids Symp Ser (Oxf) 487-488 (2008).

Seccareccia F, Zuccaro P, Pacifici R, Meli P, Pannozzo F *et al.*. Serum cotinine as a marker of environmental tobacco smoke exposure in epidemiological studies: the experience of the MATISS project. Eur J Epidemiol 18, 487-492 (2003)

Semenkovich CF, Ostlund RE, Jr., Olson MO and Yang JW. A protein partially expressed on the surface of HepG2 cells that binds lipoproteins specifically is nucleolin. Biochemistry 29, 9708-9713 (1990).

Seo JK, Choi SY, Kim Y, Baek SH, Kim KT *et al.*. A peptide with unique receptor specificity: stimulation of phosphoinositide hydrolysis and induction of superoxide

generation in human neutrophils. J Immunol 158, 1895-1901 (1997).

Seong MW, Hwang JH, Moon JS, Ryu HJ, Kong SY *et al.*. Neonatal hair nicotine levels and fetal exposure to paternal smoking at home. Am J Epidemiol 168, 1140-1144 (2008).

Seong MW, Nam MH, Ryu HJ, Kong SY, Myung SK *et al.*. The comparison of two smoking biomarkers in various biological samples. Clin Chim Acta 383, 180-181 (2007).

Sexton K, Adgate JL, Church TR, Hecht SS, Ramachandran G *et al.*. Children's exposure to environmental tobacco smoke: using diverse exposure metrics to document ethnic/racial differences. Environ Health Perspect 112, 392-327 (2004).

Shaikh NA, Ge J, Zhao YX, Walker P and Drebot M. Development of a novel, rapid, and sensitive immunochromatographic strip assay specific for West Nile Virus (WNV) IgM and testing of its diagnostic accuracy in patients suspected of WNV infection. Clin Chem 53, 2031-2034 (2007).

Shigenaga MK, Trevor AJ and Castagnoli N, Jr. Metabolism-dependent covalent binding of (S)-[5-3H]nicotine to liver and lung microsomal macromolecules. Drug Metab Dispos 16, 397-402 (1988).

Shoaib M and Stolerman IP. Plasma nicotine and cotinine levels following intravenous nicotine self-administration in rats. Psychopharmacology (Berl) 143, 318-321 (1999).

Smith GP. Filamentous fusion phage: novel expression vectors that display cloned antigens on the virion surface. Science 228, 1315-1317 (1985).

Smith GP. Surface presentation of protein epitopes using bacteriophage expression systems. Curr Opin Biotechnol 2, 668-673 (1991).

Smith GP and Scott JK. Libraries of peptides and proteins displayed on filamentous phage. Methods Enzymol 217, 228-257 (1993).

Smothers JF, Henikoff S and Carter P. Tech.Sight. Phage display. Affinity selection from biological libraries. Science 298, 621-622 (2002).

Soundararajan S, Chen W, Spicer EK, Courtenay-Luck N and Fernandes DJ. The nucleolin targeting aptamer AS1411 destabilizes Bcl-2 messenger RNA in human breast cancer cells. Cancer Res 68, 2358-2365 (2008).

Soundararajan S, Wang L, Sridharan V, Chen W, Courtenay-Luck N *et al.*. Plasma membrane nucleolin is a receptor for the anticancer aptamer AS1411 in MV4-11 leukemia cells. Mol Pharmacol 76, 984-991 (2009).

Syed S, Schuyler PD, Kulczycky M and Sheffield WP. Potent antithrombin activity and delayed clearance from the circulation characterize recombinant hirudin genetically fused to albumin. Blood 89, 3243-3252 (1997).

Szardenings M. Phage display of random peptide libraries: applications, limits, and potential. J Recept Signal Transduct Res 23, 307-349 (2003).

Szurdoki F, Szekacs A, Le HM and Hammock BD. Synthesis of haptens and protein conjugates for the development of immunoassays for the insect growth regulator fenoxycarb. J Agric Food Chem 50, 29-40 (2002).

Tanaka Y, Honda T, Matsuura K, Kimura Y and Inui M. In vitro selection and characterization of DNA aptamers specific for phospholamban. J Pharmacol Exp Ther 329, 57-63 (2009).

Tang D, Phillips DH, Stampfer M, Mooney LA, Hsu Y *et al.*. Association between carcinogen-DNA adducts in white blood cells and lung cancer risk in the physicians health study. Cancer Res 61, 6708-6712 (2001).

Tang D, Warburton D, Tannenbaum SR, Skipper P, Santella RM *et al.*. Molecular and genetic damage from environmental tobacco smoke in young children. Cancer Epidemiol Biomarkers Prev 1999;8:427-31

Trill JJ, Shatzman AR and Ganguly S. Production of monoclonal antibodies in COS and CHO cells. Curr Opin Biotechnol 6, 553-560 (1995).

Tuerk C and Gold L. Systematic evolution of ligands by exponential enrichment: RNA ligands to bacteriophage T4 DNA polymerase. Science 249, 505-510 (1990).

Tuomi T, Johnsson T and Reijula K. Analysis of nicotine, 3-hydroxycotinine, cotinine, and caffeine in urine of passive smokers by HPLC-tandem mass spectrometry. Clin Chem 45, 2164-2172 (1999).

Ulrich H, Ippolito JE, Pagan OR, Eterovic VA, Hann RM *et al.*. In vitro selection of RNA molecules that displace cocaine from the membrane-bound nicotinic acetylcholine receptor. Proc Natl Acad Sci U S A 95, 14051-14056 (1998).

Ulrich H, Magdesian MH, Alves MJ and Colli W. In vitro selection of RNA aptamers that bind to cell adhesion receptors of Trypanosoma cruzi and inhibit cell invasion. J Biol Chem 277, 20756-20762 (2002).

Van der Merwe PA, Barclay AN, Mason DW, Davies EA, Morgan BP *et al.*. Human cell-adhesion molecule CD2 binds CD58 (LFA-3) with a very low affinity and an extremely fast dissociation rate but does not bind CD48 or CD59. Biochemistry 33, 10140-10160 (1994).

Walsh G. Biopharmaceutical benchmarks. Nat Biotechnol 18, 831-833 (2000).

Walter G, Konthur Z and Lehrach H. High-throughput screening of surface displayed gene products. Comb Chem High Throughput Screen 4, 193-205 (2002).

Whincup PH, Gilg JA, Emberson JR, Jarvis MJ, Feyerabend C *et al.*. Passive smoking and risk of coronary heart disease and stroke: prospective study with cotinine measurement. BMJ 329, 200-205 (2004).

Williams DL, Jr., Murphy KL, Nolan NA, O'Brien JA, Lis EV, Jr. *et al.*. Pharmacology of L-744,453, a novel nonpeptidyl endothelin antagonist. Life Sci 58, 1149-1157 (1996).

Wong SC, Tesanovic M and Poon MC. Detection of two abnormal hemoglobins, Hb Manitoba and Hb G-Coushatta, during analysis of glycohemoglobin (A1c) by high-performance liquid chromatography. Clin Chem 37, 1456-1459 (1991).

Yang D, Chen Q, Gertz B, He R, Phulsuksombati M *et al.*. Human dendritic cells express functional formyl peptide receptor-like-2 (FPRL2) throughout maturation. J Leukoc Biol 72, 598-607 (2002).

Yin P, Jiang CQ, Cheng KK, Lam TH, Lam KH *et al.*. Passive smoking exposure and risk of COPD among adults in China: the Guangzhou Biobank Cohort Study. Lancet 370,

751-757 (2007).

국문초록

코티닌은 니코틴의 주요 대사산물로 흡엽에 대한 바이오마커로 널리 사용되는 물질로, 혈청 코티닌의 농도는 우리 몸이 직접 혹은 간접 흡연에 대하여 노출된 정도를 반영한다. 최근 간접흡연에 대한 다각도의 연구에 따르면, 간접 흡연이 직접 흡연과 비슷한 수준으로 심장질환, 폐질환, 종양성 질환에 대한 주요 위험인자로 작용하고 있음을 알 수있다. 그러나 기존의 코티닌 정량을 위한 효소면역법들은 그 감도가 낮아 간접 흡연에 노출된 정도를 정량화 하는 것에 한계가 있으므로 실질적으로 아직까지 간접 흡연 정도를 고속대량 스크리닝 방법으로 측정하기가 불가능하였다. 이에 파지 디스플레이 방법을 이용하여 제작한 항 코티닌 단일클론 항체를 이용하여 고감도의 효소면역법을 개발하였고, 임상시료와 동물 모델을 이용하여 개발한 효소면역법의 효용성과 민감도 및 정확도를 평가하였다. 효소면역법의 최소 정량적 검출한계와 cut-off 값은 각각 1 ng/mL과 5.1 ng/mL이었고, 세 가지 서로 다른 농도의 퀄리티 콘트롤 시료를 이용하여 측정한 intra-, inter-assay precisions 값은 각각 3.8–13.5%와 14.0–15.0%이었다. 트랜스-3'-하이드록시 코티닌이나 아나바신 및 다른 혈청 물질에 대한 의미있는 간섭현상은 측정되지 않았다. 그리고 서로 다른 흡연 패턴을 가지고 있는 36 명의 혈청을 재작한 효소면역법로 분석 한 결과 비 흡연자로부터 직접 흡연자뿐만 아니라 간접

흡연자를 구별 가능하였다. 또한 동일한 농도의 코티닌을 포함한 사람 혈청시료을 재작한 효소면역법과 LC/MS로 측정하였을 때, 낮은 코티닌 농도의 혈청시표에서 LC/MS보다 더 정확하고 재연성있는 결과가 도출됨을 확인하였다. 마지막으로 간접흡연 혹은 직접 흡연을 야기할 수 있도록 적정량의 니코틴을 투여한 쥐로부터 시간에 따라 혈청을 얻고 이를 재작한 효소면역법으로 분석한 결과, 혈청 내 코티닌의 kinetics를 확인할 수 있었을뿐만 아니라 두 그룹의 쥐가 서로 구분이 됨을 확인하였다.

코티닌 진단용 효소면역법의 개발과 더불어 항 코티닌 항체의 또 다른 적용방법으로서 코티닌 결합물질에 대한 체내 및 체외 운반 시스템을 개발하였다. 이 시스템은 단백질이나 펩타이드 등의 물질을 링커를 매개로 코티닌에 접합한 뒤, 항 코티닌 항체와 더불어 복합체를 형성하도록 고안되었다. 이 시스템의 가장 큰 특징은 코티닌 접합물질의 특정 타겟에 대한 반응성과 생리적 활성등의 고유 성질과 항체의 긴 반감기, 항체 의존성 세포독성, 보체 의존성 세포독성 등의 고유 성질을 모두 유지 가능하다는 점에 있다. 이 시스템의 코티닌 접합물질에 대한 체외 운반체로서의 기능을 확인하기 위하여 폐혈증에 치료효과가 있는 펩타이드인 WKYMVm-NH_2을 코티닌에 접합하였다. 그 결과, WKYMVm-NH_2가 코티닌에 접합 후 항 코티닌 항체와 복합체를 형성할 경우에 고유의 반응성 및 활성을 그대로 유지가 되었고, 짧았던 생체 내 반감기가 극적으로 증가하는 것을 알 수 있었다. 또한 폐혈증모델 쥐를 이용한 효능 실험에서 WKYMVm-NH_2만 투여한 폐혈증모델

쥐에 비하여 복합체 형태로 투여한 폐혈증모델 쥐의 생존률이 35% 이상 증가하는 것을 확인하였다. 다음으로 이 시스템의 체내 운반체로서의 기능을 확인하기 위하여 압타머를 코티닌에 접합하였고, 압타머가 접합된 코티닌과 항 코티닌 항체 복합체가 다양한 생물학적 분석 및 실험에 어피니티 유닛으로 사용될 수 있는지를 알아보았다. 이를 위해 항 코티닌 항체와 안정적인 구조를 형성 가능하도록 암타머의 5' 끝부분에 코티닌을 레이블링하는 방법을 고안하였고, 이 방법을 통하여 AS1411와 pegaptanib 압타머를 각각 코티닌에 접합하였다. 각 복합체를 다양한 실험에 적용하여 본 결과, 코티닌과 AS1411 접합체와 항 코티닌 항체 복합체는 면역블롯팅, 면역침강법 및 유세포 분석에서 어피니티 유닛으로써 성공적으로 작용하였고, 코티닌과 pegaptanib 접합체와 항 코티닌 항체 복합체는 효소면역측정법에 적용이 가능하였다.

결론적으로 파지 디스플레이 방법으로 개발한 고 친화도의 항 코티닌 항체를 이용하여 간접 흡연을 측정 가능한 고속 대량 스크리닝 방법의 개발 및 펩타이드나 압타머에 대한 체내 및 체외 운반 시스템으로 쓰일 수 있는 단일 플랫폼을 구축하였다.

주요어 : 코티닌; 간접 흡연; 파지 디스플레이; 단일 클론 항체; 면역 측정법; 펩타이드; 약물운반시스템; 압타머; 어피니티 유닛

학번 : 2006-30539